Meteorological Precursors to the Explosive Intensification of the *QE II* Storm

JOHN R. GYAKUM

Department of Meteorology, McGill University, Montreal, Canada

(Manuscript received 2 July 1990, in final form 22 October 1990)

ABSTRACT

The objective of this research is to define the meteorological conditions *prior* to the explosive development of the *QE II* storm. By using conventional data and detailed McIDAS satellite imagery we document the genesis of this storm along a preexisting line of active surface frontogenesis, 12 h before the onset of its extraordinarily rapid 24-h central pressure fall of nearly 60 mb. This particular surface cyclone, having formed on the western edge of a convective complex, is shown to be a lower-tropospheric warm-core phenomenon at the time of its birth. During the first 12 h of existence, the cyclone deepened 7 mb and its surface relative vorticity increased to 17×10^{-5} s^{-1}. The cyclone had intensified sufficiently, after only 6 h, to have developed the characteristic pattern of strong cold and warm frontogenesis regions. During the 24-h period of explosive intensification, a strong midtropospheric trough interacted with the already well-developed surface cyclone. This period corresponds to the cyclone's transformation into a larger and deeper system.

The particular midtropospheric trough is traced on its southeastward path from the Canadian Northwest Territories until it interacts with the *QE II* storm during its explosive intensification. This upper-tropospheric trough is also found to be associated with another distinct and intensifying surface cyclone, whose identity is maintained until after the initiation of the *QE II* storm's explosive intensification. We demonstrate that this particular surface cyclone has a deep, cold-core structure during the initial 12 h of the separate and shallow *QE II* storm.

This documentation of a separate, independent origin and development for each of the surface and upper-tropospheric cyclonic disturbances involved in this explosive cyclone intensification motivates us to suggest a two-stage process of cyclone development that may be unique to the explosively developing cyclone. The first stage involves the genesis and development of the surface cyclone. For this particular case, the surface cyclogenesis occurs as a shallow frontal wave that develops independently of an upper-tropospheric trough. This frontal wave develops strong winds of 18 m s^{-1}, extending to 300 km south of its center, and a sufficient amount of cyclonic vorticity (17×10^{-5} s^{-1} in this case) to dramatically enhance the surface response to the approach of the upper-tropospheric trough. The interaction of the upper-tropospheric trough and the strong surface cyclone constitutes the onset of stage two of the development process that corresponds to the cyclone's explosive intensification period.

This research suggests that not all cyclogenesis can be regarded as a classical type "B" development in which the surface cyclone forms in response to an approaching upper-tropospheric trough. Rather, we suggest that a surface cyclone's explosive intensification may typically involve the interaction of separate surface and upper-tropospheric cyclonic disturbances, each of whose development may be substantial enough, before their interaction, to warrant their individual examination.

1. Introduction

The rapidly developing cyclone of September 1978, commonly called the *QE II* storm because of its battering of the ocean liner, has been discussed extensively in the literature (Gyakum 1983a,b; Anthes et al. 1983; Uccellini 1986; Kuo et al. 1990a). Previous study of this case and indeed, much of the explosive cyclogenesis research, has concentrated on the 24-h period of the cyclone's most rapid intensification (see, for example, Roebber 1984; Sanders 1986; and Whitaker et al. 1988). The particular central pressure fall of nearly 60 mb during this 24-h period in the case of the *QE II* storm easily qualifies the cyclone as being one of the most extreme of the "bomb" events (Sanders and Gyakum 1980).

However, this surface low was already well developed at the onset of the 24-h period of explosive deepening. Gyakum's (1983a) mesoscale surface wind analysis at this time, 1200 UTC 9 September, shows a relative vorticity of 17×10^{-5} s^{-1} and associated 18 m s^{-1} surface winds in the vicinity of its center. Such strong winds extended to 300 km south of the center, showing the system's strength. Figure 1 illustrates this substantial vorticity enhancement during the first 12 h of the cyclone's existence. Although the low's central pressure of 1004 mb appears benign, its geostrophic relative vorticity of 30×10^{-5} s^{-1} at the onset of explosive deepening suggests considerable antecedent development of this cyclone.

Corresponding author address: Prof. John R. Gyakum, Dept. of Meteorology, McGill University, 805 Sherbrooke Street West, Montreal Quebec H3A 2K6, Canada.

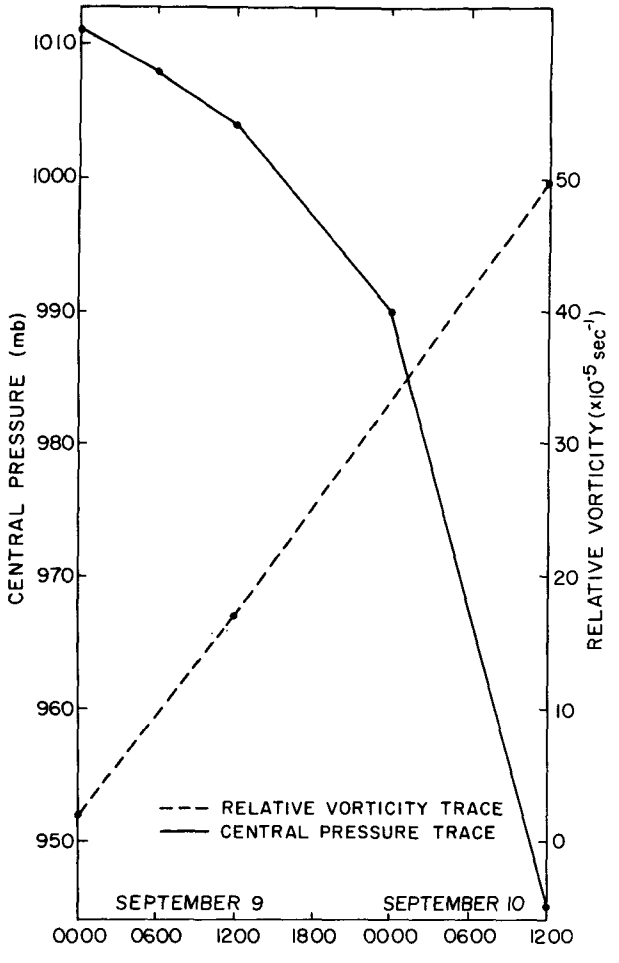

FIG. 1. Surface relative vorticity (dashed, 10^{-5} s^{-1}) and central pressure (solid, mb) traces of the *QE II* cyclone for the 36-h period beginning at 0000 UTC 9 September 1978.

This antecedent development, its associated physical processes and its potential importance for the explosive cyclogenesis problem, have not been emphasized in research concerning this case. For example, Uccellini (1986) focuses upon the role of the upper-level trough and its interaction with the surface system during its 24-h period of most rapid intensification. Anthes et al. (1983) and Kuo et al. (1990a) use numerical simulations to study this 24-h period of explosive development that begins at 1200 UTC 9 September. These simulations were all initialized at this time; therefore, the physical mechanisms of this potentially important antecedent cyclone intensification were not studied.

The primary purpose of this study is to give a complete physical description of the relevant meteorological processes *prior* to the explosive intensification phase of the *QE II* cyclone. Particular emphasis will be placed upon the documentation and diagnosis of the surface cyclone development from the time of its initial formation at 0000 UTC 9 September, until the onset of its explosive intensification at 1200 UTC 9 September. The documentation of this early cyclogenesis will be carried out with the aid of detailed satellite imagery to supplement the surface data compiled by Gyakum (1983a). This particular time period will be defined as the stage I, or antecedent development, phase of the *QE II* cyclone's life cycle.

The importance of such antecedent development for explosive cyclogenesis is clear. The frictionless vorticity equation in pressure coordinates may be expressed as

$$\frac{\partial(\zeta+f)}{\partial t} = -\mathbf{V}\cdot\nabla(\zeta+f) - \omega\frac{\partial\zeta}{\partial p} - (\zeta+f)\nabla\cdot\mathbf{V} - \mathbf{k}\cdot\left(\nabla\omega\times\frac{\partial\mathbf{V}}{\partial p}\right) \quad (1)$$

where ζ is the vertical component of relative vorticity, f is the Coriolis parameter, $\mathbf{V}$ and ω are the respective horizontal and vertical wind components. If we assume that the vorticity maximum is located at the cyclone center, the horizontal advection of vorticity vanishes at the center. Furthermore, the tilting of the horizontal components of vorticity into the vertical is small (surface vertical motions are negligible), and (1), valid for the storm center, reduces to

$$\frac{\partial(\zeta+f)}{\partial t} = -(\zeta+f)\nabla\cdot\mathbf{V}. \quad (2)$$

Thus, surface vorticity increases near the low center are typically dominated by the product of surface convergence and absolute vorticity. A time integration of (2) yields an exponential growth of absolute vorticity in the presence of constant convergence. A finite surface vorticity enhancement prior to the onset of a particular period of intensification would, therefore, enhance dramatically such intensification. Furthermore, if convergence increases during cyclone development, the growth of surface vorticity would exceed the exponential rate; such a scenario offers a plausible explanation for explosive cyclogenesis.

Palmén and Newton (1969, pp. 319–320) recognized that antecedent surface vorticity development is a potentially important factor in rapid cyclone intensification by using Eq. (2) to state that the most rapid cyclonic development is "in part related to the circumstance that the increase of vorticity due to convergence is directly proportional to vorticity itself or to the preexisting circulation that is always cyclonic at any surface front." However, much of the published literature concerning extratropical cyclogenesis during the past ten years has emphasized the dominant role of the 500-mb trough in forcing rapid cyclone intensification with little discussion of the development being enhanced by the strength of the surface circulation at the onset of most rapid development. Hoskins et al. (1985) describe cyclogenesis as consisting of an upper-air positive isentropic potential-vorticity anomaly initially interact-

ing with a low-level baroclinic zone without appreciable circulation. Sanders (1986) emphasizes the relationship of explosive cyclone intensification to the amplitude of the 500-mb cyclonic vorticity advection.

The antecedent surface vorticity enhancement may have been crucial to the subsequent period of explosive intensification, during which a strong upper-tropospheric trough began to influence this vorticity-rich surface environment. Such vorticity development may be a key process in the antecedent *conditioning* of the lower troposphere that provides such an extraordinary response to baroclinic forcing, as suggested by Sanders (1986), and as a scientific hypothesis for the Experiment on Rapidly Intensifying Cyclones over the Atlantic (ERICA; Hadlock and Kreitzberg 1988).

Research concerning rapid cyclogenesis has typically emphasized the reduction of static stability as the key conditioning precursor that provides a large response to baroclinic forcing (see, for example, Reed and Albright 1986). Indeed, we present evidence in this paper that nearly saturated air with moist, adiabatic lapse rates are located near the incipient cyclone center. This suggests that moist upright convection may have acted to adjust the environment to a moist neutral state. Convective echoes with tops up to 13 km, in the vicinity of the incipient cyclone, have been shown by Gyakum (1983a). Tracton (1973) has also shown moist convective elements to exist near the centers of young baroclinic cyclones. Generally weak stratification in explosively developing cyclones has been documented by Sanders and Gyakum (1980) and Rogers and Bosart (1986). Recent work by Emanuel (1988) suggests that slantwise moist convection in ascent regions of extratropical cyclones may act to neutralize the instability that is generated by the cyclone-scale ascent. Thus, the broad regions of slightly stable stratification in the vertical that have been shown by earlier studies may be regions in which slantwise moist convection has adjusted the lapse rates along absolute momentum surfaces (Emanuel 1983) to conditional neutrality. We suggest in this paper that the explosive cyclogenesis process may uniquely include *both* antecedent destabilization and vorticity enhancement in the conditioning process.

Though the relative importance of particular cyclogenetic processes varies with case, the incipient development of the *QE II* storm has some important similarities to other "bombs" described in the literature. The low developed along a strong and intensifying surface front and had significant cumulus convection associated with it. Such precursors were associated with the early and explosive deepening of the Presidents' Day cyclone studied by Bosart (1981) and Bosart and Lin (1984), and in cases studied by Reed and Albright (1986) and Gyakum and Barker (1988). The *QE II* cyclone may be documented in two stages. The first stage (0000 UTC 9 September–1200 UTC 9 September) consists of the low's first appearance along a shallow preexisting, intensifying hyperbaroclinic zone. The second stage (1200 UTC 9 September–1200 UTC 10 September) is the explosive cyclogenesis that consists of the interaction of a transient upper-tropospheric trough with the vorticity-rich surface boundary layer.

An additional objective of this study is to document the interaction of this transient upper trough with *two* separate surface cyclones, a relevant fact not previously discussed in the literature. Uccellini (1986) has pointed to this trough, and its associated jet, as influencing the explosive development of the *QE II* cyclone. We will show this upper-level vorticity maximum to have been actively associated with another deepening surface cyclone that continued to exist until after 1200 UTC 9 September. The formation of the separate surface cyclone in New Jersey at 0000 UTC 9 September, and its stage I development, concurrent with the distinct and deep cyclone in Canada, suggests the former system's independence from the upper trough. This southern surface cyclone, which became the *QE II* storm, remains a shallow disturbance, not coupled to the upper trough, throughout its stage I intensification period. It is not until after this period, and after the Canadian surface low lost its identity, that the *QE II* cyclone interacted with this upper trough, and intensified explosively. Sanders (1988) has noted that individual 500-mb troughs may interact with multiple surface cyclones during their lifetimes.

We will describe the detailed synoptic-scale and mesoscale features associated with the *QE II* storm's initial development near Atlantic City, New Jersey at 0000 UTC 9 September. We will follow the evolution of this mesoscale vortex eastward to its position south of Cape Cod, Massachusetts at 1200 UTC 9 September with the aid of detailed surface analyses and satellite imagery. This time, corresponding to the onset of the cyclone's second stage of development, is also the time at which the numerical simulations described by Anthes et al. (1983) and Kuo et al. (1991a) were initialized. Motivation is given in this study for future modeling work that concentrates on simulating the full life cycle of the explosively developing cyclone, including its antecedent conditioning phase.

The database used to document the first stage of development of the *QE II* storm is described in section 2. Section 3 describes the synoptic-scale environment and associated quasi-geostrophic diagnosis. The mesoscale features of the surface low are discussed in section 4, with a particular emphasis on the antecedent development of the surface front. Section 5 consists of the concluding discussion.

2. Database and diagnostic calculations

The data used in this study include hourly land and marine surface observations, and the upper-air observations of rawinsondes and commercial aircraft reports as compiled by Gyakum (1983a). The National Me-

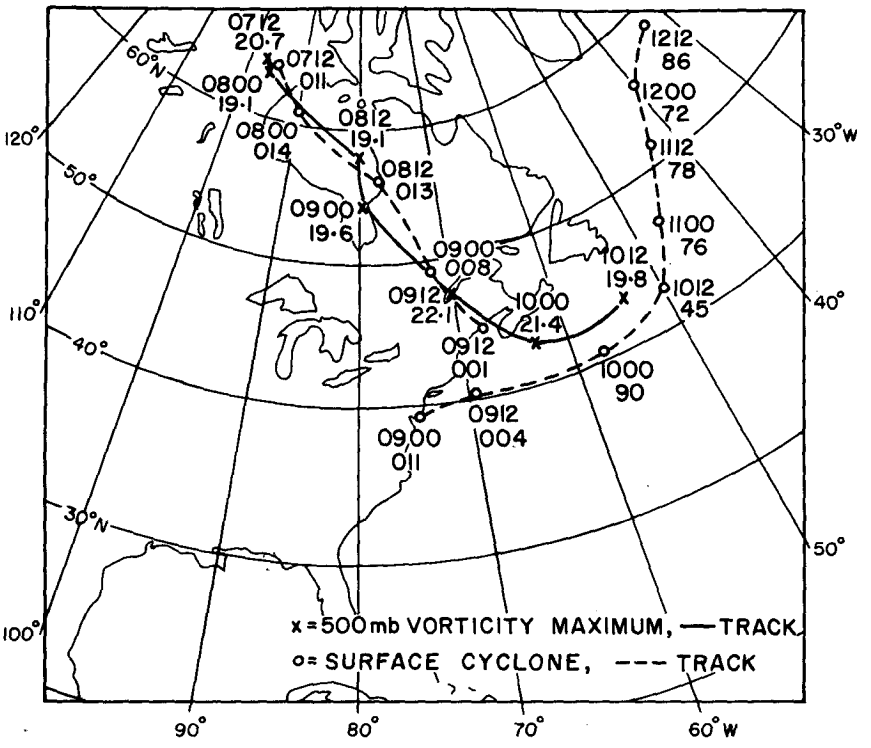

FIG. 2. Tracks of surface cyclones (dashed) and 500-mb absolute vorticity maxima (solid). Open circles show the 12-h positions of surface cyclones; dates and times are shown (0900 = 9 September at 0000 UTC), along with central pressures (mb, with the hundreds or thousands digit omitted). The vorticity maxima are also shown each 12 h until 1200 UTC 10 September with the times and absolute vorticity (10^{-5} s^{-1}) shown.

teorological Center's (NMC) surface maps and NMC analyses, interpolated to a 381-km octagonal grid and compiled on a compact disk (Mass et al. 1987) for the surface, 850, 500, and 200 mb, are also used in this study. Additionally, film loops and GOES satellite imagery were constructed with the aid of the Man-computer Interactive Data Access System (McIDAS) at the Space Science and Engineering Center of the University of Wisconsin.

The quasi-geostrophic ω equation may be expressed as

$$\left(\sigma\nabla^2 + f_0^2\frac{\partial^2}{\partial p^2}\right)\omega = -2h\nabla\cdot\mathbf{Q} \qquad (3)$$

where $h = (R/p)(p/p_0)^\kappa$, κ is the ratio of the gas constant to the specific heat at constant pressure, $p_0 = 1000$ mb, and the static stability $\sigma = h(\partial\Theta/\partial p)$, where Θ is the potential temperature averaged on a constant pressure surface and ∇ and ∇^2 are evaluated on a constant pressure surface. This particular form of the ω equation was first discussed by Hoskins et al. (1978) and Hoskins and Pedder (1980). The authors introduced the Q vector ($\mathbf{Q}$), defined as

$$\mathbf{Q} = \left(-\frac{\partial\mathbf{V}_g}{\partial x}\cdot\nabla\theta\right)\mathbf{i} + \left(-\frac{\partial\mathbf{V}_g}{\partial y}\cdot\nabla\theta\right)\mathbf{j}. \qquad (4)$$

The geostrophic wind is $\mathbf{V}_g$, the horizontal potential temperature gradient is $\nabla\theta$, and positive displacements along the x and y axes point, respectively, eastward and northward. The adiabatic, inviscid forcing for this ω equation, proportional to the divergence of $\mathbf{Q}$, is therefore shown on the right side of (3).

A measure of the geostrophic frontogenesis may be expressed as the function, G:

$$G = \frac{\mathbf{Q}\cdot\nabla\theta}{|\nabla\theta|}. \qquad (5)$$

The forcing on the right side of the quasi-geostrophic ω equation (3) is computed for the 850- and 500-mb levels. The function G is found for the manually analyzed surface sectional analyses.

These detailed analyses are based upon all available conventional surface land and ship observations. Additionally, surface winds based upon satellite scatterometer instrumentation were available at 1200 UTC 9 September. This enhanced dataset allows for a detailed documentation of the surface vortex at this time; these winds are displayed in Fig. 8 of Gyakum (1983a).

3. Synoptic-scale overview

Figure 2 shows the track of the *QE II* cyclone from its initial location west of Atlantic City, New Jersey at

0000 UTC 9 September to a position east of Greenland at 1200 UTC 12 September. The particular positions and central pressures of the system through 1200 UTC 10 September are based upon Gyakum's (1983a) detailed analyses. The subsequent locations of the cyclone, based upon NMC's final hemispheric surface analyses, show its northeastward propagation into the Norwegian Sea by 15 September. The explosive 24-h pressure fall of nearly 60 mb commenced only 12 h after its first formation. Such early maximum deepening of explosively developing lows has been found by Gyakum et al. (1989) for Pacific systems, and also by Sanders (1986) in his study of explosive cyclogenesis in the west-central North Atlantic.

The 500-mb absolute vorticity maximum track (Fig. 2) extends from the Northwest Territories at 1200 UTC 7 September southeastward to a position east of Nova Scotia at 0000 UTC 10 September. This vorticity maximum was clearly associated with the *QE II* cyclone by this time, and this interaction continued during its explosive deepening. This 500-mb trough (discussed by Uccellini 1986) existed several days prior to its association with the *QE II* storm. However, this trough was associated with the development of another well-defined, and intensifying, surface cyclone, until after 1200 UTC 9 September, when its southeastward track ends south of Nova Scotia. This surface cyclone lost its identity in the strong, cold advection region to the northwest of the more intense *QE II* cyclone. Sanders (1988) has found that 500-mb troughs have distinctively different genesis regions from those of intense surface cyclones, and that these troughs can often be identified several days prior to surface cyclogenesis.

The processes associated with the surface cyclone intensification of each of the two systems will be compared and contrasted for the times of their concurrent existence 0000 and 1200 UTC 9 September. We will use satellite imagery, pressure and height analyses, and large-scale diagnostic calculations to describe these processes.

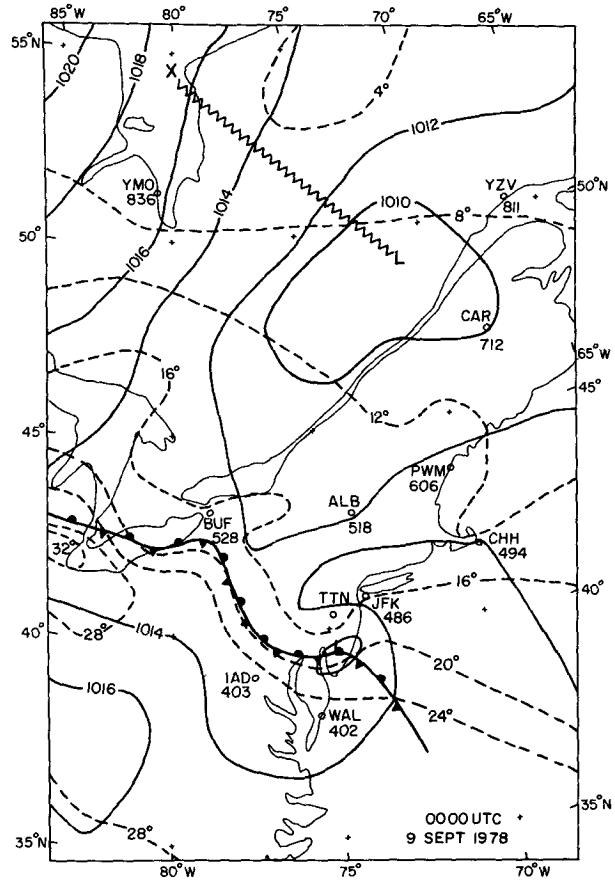

FIG. 3. Surface analysis including sea-level pressure (solid, contour interval of 2 mb), temperature (dashed, contour interval of 4°C) and fronts (conventional notation) for 0000 UTC 9 September 1978. Vorticity maximum at 500 mb is indicated by an "X"; jagged line connects this maximum with the associated surface low. Locations of soundings, described in text, are shown with World Meteorological Organization (WMO) index numbers (block numbers omitted) and three-letter aviation identifiers. Crosses indicate intersections of 5° latitude–longitude lines.

At the time of the initial development of the 1011-mb *QE II* cyclone in eastern New Jersey, 0000 UTC 9 September, there is a 1008-mb low in eastern Quebec (Fig. 3). The surface baroclinity in the vicinity of the Quebec low is approximately an order of magnitude smaller than the magnitude of the temperature contrast of 8°C (100 km)$^{-1}$ found in the midst of the storm that was to become the *QE II* cyclone. The Quebec surface low appears linked to its 500-mb vorticity maximum located 600 km to its northwest in James Bay. Indeed, this low is located on the cyclonic shear side of the 500-mb geostrophic jet (Fig. 4), and is found in the heart of the 500-mb cyclonic vorticity advection (not shown). We do, however, show in Figs. 4 and 5, the complete large-scale forcing parameter for quasi-geostrophic vertical motions, namely, $2h\nabla \cdot \mathbf{Q}$ (Eq. 3). The Q-vector convergence and the implied forcing for ascent, is associated with the Quebec low at both 500 (Fig. 4b) and at 850 mb (Fig. 5b). At 500 mb, this zone of ascent forcing is confined to Quebec and extreme northern New England while the 850-mb forcing for ascent extends from the mid-Atlantic states into New England, and is associated with warm advection. The incipient *QE II* cyclone, while located in an area of synoptic-scale warm advection and ascent at 850 mb, is located in a zone of substantial implied synoptic-scale descent at 500 mb. Despite the Quebec low's intensification at this time, its weak environmental surface baroclinity precludes any analysis of a surface front in its vicinity. The *QE II* low, on the other hand, is located along a strong and intensifying surface front.

The 4-km resolution infrared enhanced satellite image (Fig. 6) for this time suggests high and deep cloudiness throughout northern New England, eastern Quebec, and New Brunswick. This cloudiness is consistent with the deep quasi-geostrophic forcing for ascent sug-

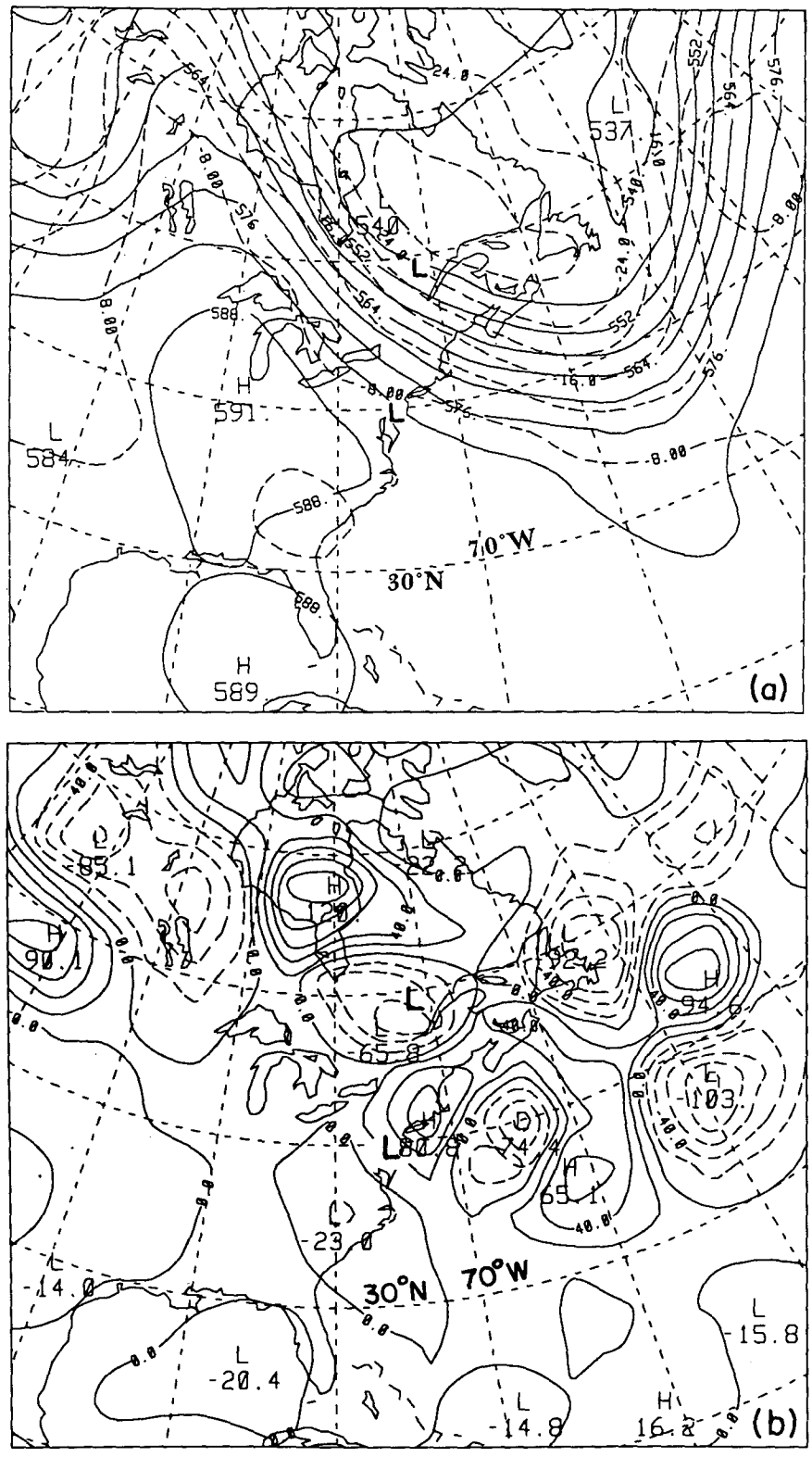

FIG. 4. (a) Fields of 500-mb geopotential height (solid, contour interval of 6 dam) and temperature (dashed, contour interval of 4°C) for 0000 UTC 9 September 1978. (b) Field of $(2h\nabla \cdot \mathbf{Q})$ at 500 mb. (The contour interval is 20×10^{-16} mb^{-1} s^{-3}.) Dashed contours indicate convergence of the Q vector. Locations of two surface lows seen in Fig. 3 are shown as "L's." Latitude and longitude lines are shown each 10°.

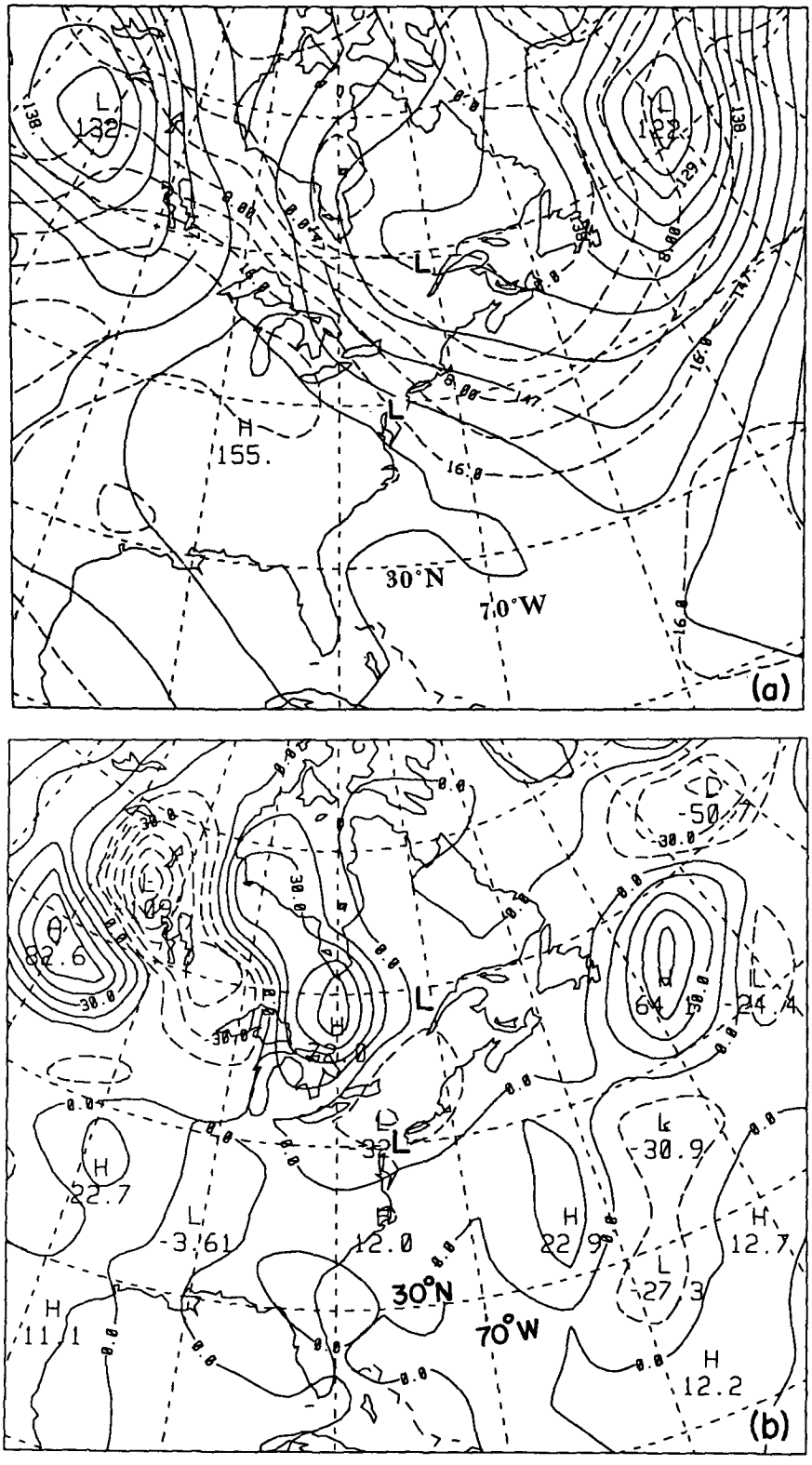

FIG. 5. (a) Fields of 850-mb geopotential height (solid, contour interval of 3 dam) and temperature (dashed, contour interval of 4°C) for 0000 UTC 9 September 1978. (b) Field of $(2h\nabla \cdot \mathbf{Q})$ at 850 mb. (The contour interval is 15×10^{-16} mb^{-1} s^{-3}.) Dashed contours indicate convergence of the Q vector. Locations of two surface lows seen in Fig. 3 are shown as "L's." Latitude and longitude lines are shown each 10°.

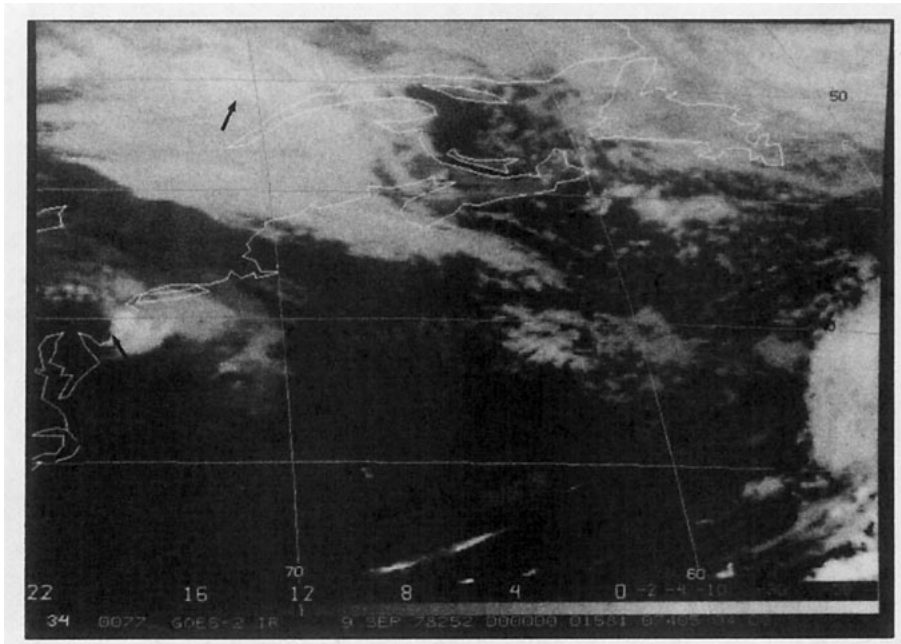

FIG. 6. GOES infrared satellite image for 0000 UTC 9 September 1978. McIDAS enhancement temperature scale (°C) is shown at the bottom of the image. Arrows point to the positions of surface lows.

gested by Figs. 4 and 5, and is associated with the Quebec surface low. The cloudiness to the south, extending from southern New England into southern New York state, is considerably shallower with cloud top temperatures no colder than 8°C; therefore, given the environmental stratification, cloud tops are no higher than approximately 800 mb. The incipient *QE II* cyclone, located along the strong surface front in New Jersey (Fig. 3), is also associated with a developing mesoscale convective system with cloud tops extending to above 13 km (see Fig. 4 of Gyakum 1983a). Figure 6 shows a line of convective clouds extending westward from the incipient surface low along the frontal system. The sounding at Caribou, Maine (CAR, Fig. 7a), located approximately 300 km southeast of the Quebec low (Fig. 3), is located within the northern cloud mass (Fig. 6). Layers of nearly saturated air extend from below 700 to 500 mb in this sounding. The Chatham, Massachusetts (CHH) sounding (Fig. 7b) located to the south in the region of shallow low cloud (Fig. 6) shows evidence of subsidence inversions near 800 and 600 mb. The highest level at which the relative humidity exceeds 75% is at 894 mb. The JFK Airport sounding (74 486, Fig. 7c), approximately 150 km to the northeast of the incipient *QE II* cyclone, on the cold side of the surface front, reveals a nearly saturated, moist-adiabatic lapse rate above the frontal zone, between 850 and 500 mb. This observation suggests that moist convection had been acting to adjust the stratification to a moist neutral state. At this time, Trenton, New Jersey, 100 km to the southwest of JFK, and 500 km to the north of the *QE II* cyclone, was reporting a moderate thunderstorm with a surface temperature of 13°C and a 5 m s^{-1} northeast wind. The evidence suggests that Trenton was experiencing deep convection based above the shallow frontal zone. All of this mesoscale convective activity in the vicinity of the surface front was occurring in an environment of lower-tropospheric synoptic-scale ascent, and synoptic-scale 500-mb descent. Uccellini (1986, his Fig. 4c) shows 300-mb winds to be convergent in this region suggesting upper-tropospheric descent.

To examine in more detail the vertical motions at 0000 UTC 9 September, we present vertical profiles of kinematically computed fields in Fig. 8. These profiles were computed directly from significant-level wind observations found at the vertices of the triangles. This technique, based upon Bellamy's (1949) work, has also been used by Bosart and Sanders (1981) in their study of the 1977 Johnstown flood event. The winds, typically observed at 30-mb intervals, were used between the surface and 100 mb to find the vertical profile of divergence in the triangle, from which omega is computed kinematically. We neglect the local pressure tendency in the calculation, as its magnitude is only 10^{-4} mb s^{-1}. The result of this calculation is found in the "uncorrected" omega profile. A constant correction is applied to the divergence profile (O'Brien 1970) so that its vertical integral between the surface and 100 mb is zero. The resulting kinematic profile of omega is shown in the "corrected" curve.

We have also used the winds observed at each of the vertices to compute the circulation, and its area-averaged counterpart, the vorticity over the triangle.

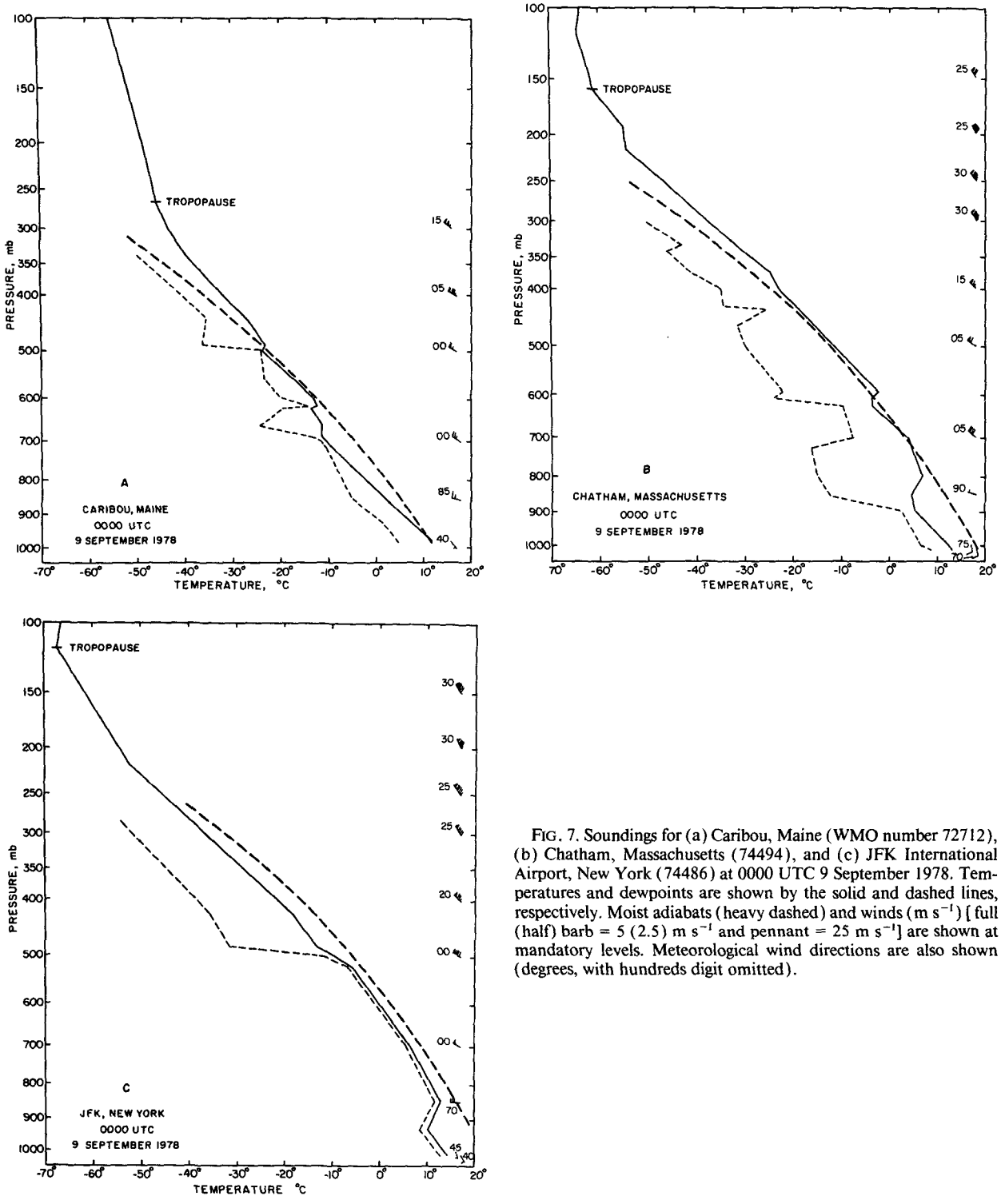

FIG. 7. Soundings for (a) Caribou, Maine (WMO number 72712), (b) Chatham, Massachusetts (74494), and (c) JFK International Airport, New York (74486) at 0000 UTC 9 September 1978. Temperatures and dewpoints are shown by the solid and dashed lines, respectively. Moist adiabats (heavy dashed) and winds (m s^{-1}) [full (half) barb = 5 (2.5) m s^{-1} and pennant = 25 m s^{-1}] are shown at mandatory levels. Meteorological wind directions are also shown (degrees, with hundreds digit omitted).

The southernmost triangle encompassing the southeastern section of the strong surface front and its incipient surface cyclone (Fig. 8a), consisting of the vertices New York, Washington D.C. and Wallops Island, shows synoptic-scale ascent confined to the lower troposphere and capped by strong middle- and upper-tropospheric descent. This result provides independent verification of the quasi-geostrophic ascent suggested at 850 mb (Fig. 5b) and descent at 500 mb throughout this triangle (Fig. 4b). The New York, Washington,

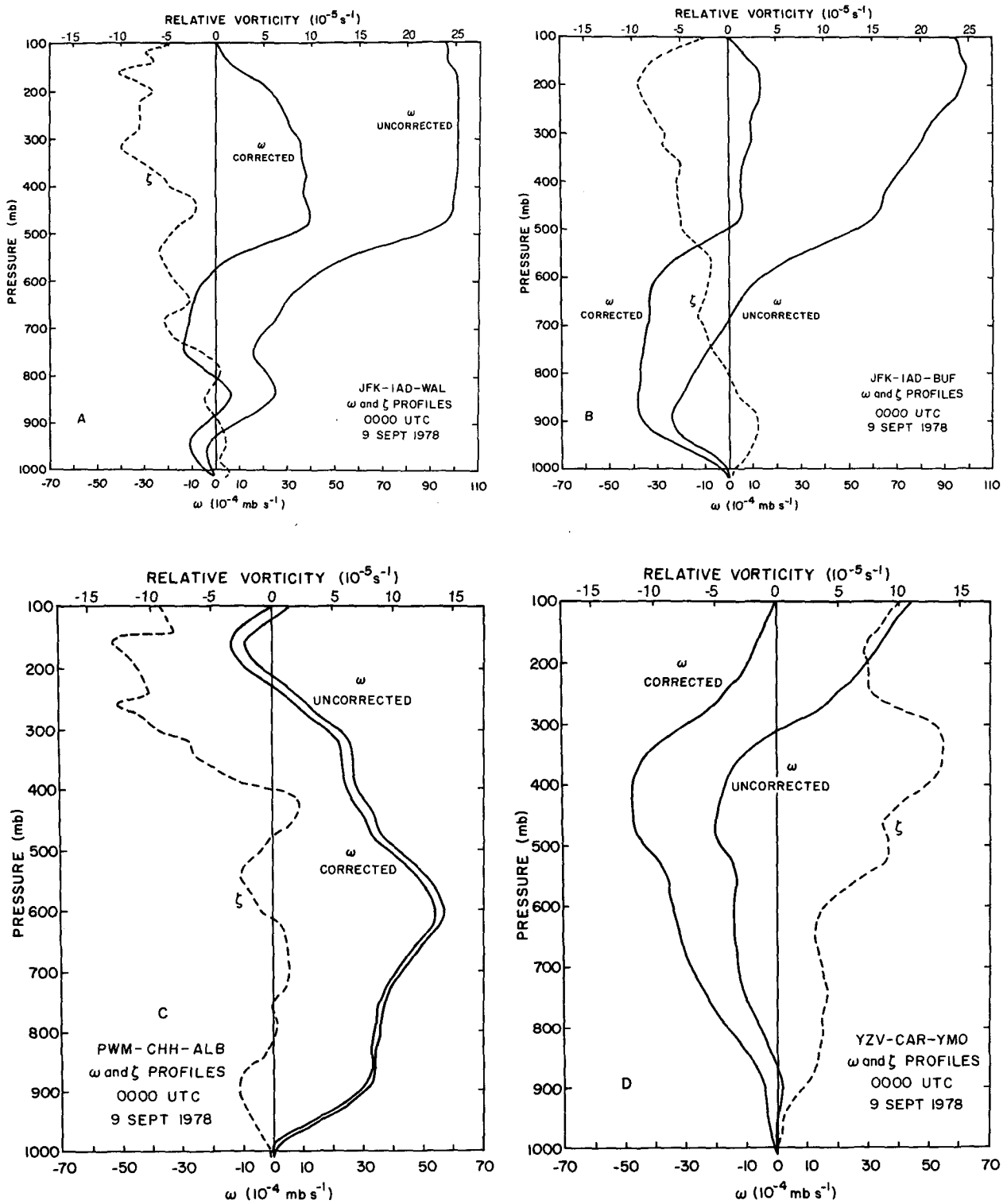

FIG. 8. Vertical profiles of kinematically computed vertical motions (solid, 10^{-4} mb s^{-1}) and vorticity ζ (dashed, 10^{-5} s^{-1}), at 0000 UTC 9 September 1978, for the triangles (a) New York (JFK), Dulles International Airport (IAD) and Wallops Island (WAL); (b) JFK, IAD and Buffalo (BUF); (c) Portland (PWM), Chatham (CHH), and Albany (ALB); (d) Sept Iles (YZV), Caribou (CAR), and Moosonee (YMO).

and Buffalo triangle (Fig. 8b) encloses the region of this strong surface front to the northwest (Fig. 3); its vorticity and vertical motions are similar in vertical structure to the Wallops Island (WAL), Washington, and New York triangle surrounding the incipient *QE II* cyclone to the southeast. Cyclonic vorticity, peaking at 5×10^{-5} s^{-1} at 920 mb is confined to the layer below 870 mb. Both regions show lower-tropospheric cyclonic vorticity capped by anticyclonic vorticity aloft. If we assume that the vertical shear of the vorticity approximates the vertical shear of the geostrophic vorticity, then the environment surrounding the front and the incipient cyclone is warm-core.

Figure 8c, showing the vertical motion in the Portland, Chatham, and Albany triangle in the heart of the clear–shallow cloud area seen in the satellite image (Fig. 6), shows deep subsidence throughout the troposphere. This result is quite consistent with the 500-mb Q-vector divergence (Fig. 4b) covering this area. Though there is synoptic-scale warm advection and convergence of the Q vectors in this area at 850 mb (Fig. 5), the small surface ridge seen in southern New England (Fig. 3) suggests lower-tropospheric subsidence. The vorticity structure, anticyclonic in the layer below 810 mb, becomes weakly cyclonic in a thin layer centered at 700 mb. Such a cold-core anticyclone structure is dynamically consistent with our description of the hydrostatically cool New England surface anticyclone seen in Fig. 3. As in Figs. 8a,b, this triangle shows strong anticyclonic vorticity in the upper troposphere.

There is little doubt, however, of the deep ascent found within the Sept Iles, Caribou, and Moosonee triangle (Fig. 8d) that surrounds the Quebec surface cyclone. The particularly strong middle-tropospheric convergence and ascent is consistent with the fact that this triangle also encloses the heart of the 500-mb cyclonic vorticity advection and Q-vector convergence (Fig. 4b) associated with the James Bay trough (Figs. 3 and 4a). The weak, nearly negligible ascent seen in the lowest 200 mb is consistent with the fact that the surface cyclone is located in an area of negligible surface and 850-mb baroclinity (Figs. 3 and 5a). The deep cold-core structure of this cyclone is confirmed by the upward increase in cyclonic vorticity.

The 1200 UTC surface chart (Fig. 9) still shows two distinct surface cyclones. The northern low has moved to a position in eastern Maine and has deepened to 1001 mb. This particular low is still associated with the 500-mb trough now only 300 km to its northwest. The developing *QE II* cyclone, located to the southeast of Cape Cod, Massachusetts, has intensified to 1004 mb. The latter cyclone is still located in a region of strong horizontal temperature contrast. This region of strong baroclinity remains behind the cold front, because of the strong sea-surface temperature gradient in this region (Fig. 10 of Gyakum 1983a). The Maine low continues to be located in a surface environment devoid of a front and any significant baroclinity.

The 500-mb height, temperature, and Q-vector forcing fields (Fig. 10) at 1200 UTC 9 September show the Maine surface low in a favorable position for continued development, downstream of the trough in the cyclonic shear region of the jet. This surface low is still located in a region of strong Q-vector convergence. However, a comparison between Figs. 4b and 10b reveals that the location of maximum quasi-geostrophic forcing for ascent has moved from a position upstream of the surface low at 0000 UTC to downstream of the low by 1200 UTC. The Q-vector convergence maximum strengthens during this 12-h period and covers much of the northwestern Atlantic basin east of 64°W at 40°N. The developing *QE II* cyclone, located in the heart of the 500-mb Q-vector divergence and subsidence, continues to be located in the anticyclonic shear side of the 500-mb jet.

Uccellini (1986) has presented apparently contrary evidence to suggest that the *QE II* cyclone is being driven by strong upper-level support at this time (1200 UTC). He bases much of his evidence on fields of 300-mb divergence and vorticity advection at 0000 and 1200 UTC 9 September (see his Fig. 4), computed from a model-based global analysis system. We show vorticity advection fields as a comparison with Uccellini's results. The NMC-based 200-mb height data allows us to compute the geostrophic absolute vorticity advection. Advection is defined in the traditional manner in the Northern Hemisphere so that positive fields correspond to cyclonic vorticity advection. These fields (Fig. 11) are similar to those of Uccellini. The 0000 UTC field shows cyclonic vorticity advection covering the entire region from the Gaspe Peninsula of Quebec southward to the Delaware, Maryland, Virginia peninsula of the United States. However, our examination of the soundings, the kinematic vertical motions, the satellite imagery and the Q-vector forcing at 500 and 850 mb has suggested that the *QE II* cyclone at 0000 UTC was located in a region of strong lower-tropospheric ascent that was capped by strong middle-tropospheric descent. The vertical structure of the surface cyclone in Quebec was markedly different with deep tropospheric ascent apparently linked with the middle- and upper-tropospheric vorticity maxima described by both this study and by Uccellini's.

The 1200 UTC field of 200-mb vorticity advection (Fig. 11b) also appears similar to the corresponding 300-mb field shown in Uccellini's (1986) Fig. 4b. The area of cyclonic vorticity advection covers much of the United States middle Atlantic coast and the Canadian Maritime provinces. This particular region of vorticity advection does not appear linked to the surface disturbance. Indeed, our more complete forcings, computed at 500 mb and shown in Figs. 4b and 10b, show a different structure from that seen in the 200-mb fields. This middle-tropospheric forcing appears more consistent with the other data describing the distinct character of each of the two surface cyclones. While it is

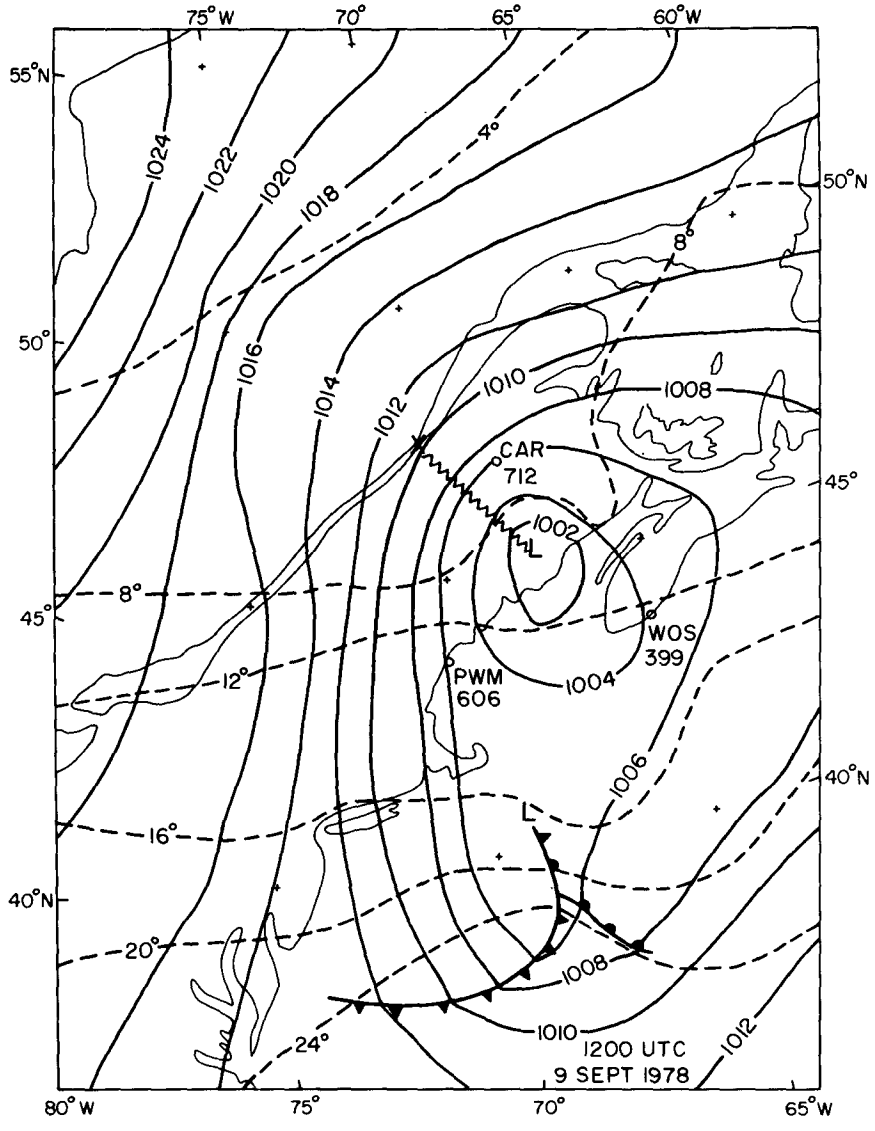

FIG. 9. As for Fig. 3, except for 1200 UTC 9 September 1978. Soundings used for Fig. 14 are also shown.

not possible to document the vertical structure of the *QE II* cyclone at 1200 UTC in as much detail as for 0000 UTC, because of its offshore location, the detailed surface analyses, 850- and 500-mb Q-vector fields and satellite imagery still allow us to deduce distinct dynamical characteristics of each surface cyclone at this later hour. The quasi-geostrophic forcing at 500 mb still suggests descent at 1200 UTC; this result will be corroborated in section 4 with satellite imagery showing cloud tops no higher than 800 mb.

The 850-mb height, temperature and quasi-geostrophic Q-vector forcing fields at 1200 UTC 9 September (Fig. 12) show a closed cyclone associated with the Maine surface low with strong geostrophic cold advection extending throughout New England, southern Ontario, and Quebec to offshore of southern New England and the middle Atlantic states. The pattern of Q-vector forcing follows closely this thermal advection field with strong Q-vector divergence and convergence associated, respectively, with cold and warm advection. The couplet of 850-mb forcing has strengthened since 0000 UTC as both surface cyclones have intensified during this 12-h period. The strong warm advection and Q-vector convergence is concentrated directly east of the developing *QE II* cyclone along its subsequent path and along the zone of strong surface (Fig. 9) and 850-mb baroclinity.

The 1200 UTC infrared satellite image (Fig. 13) suggests consistency with our concurrent 850- and 500-mb diagnostic fields in that cold high clouds are shown

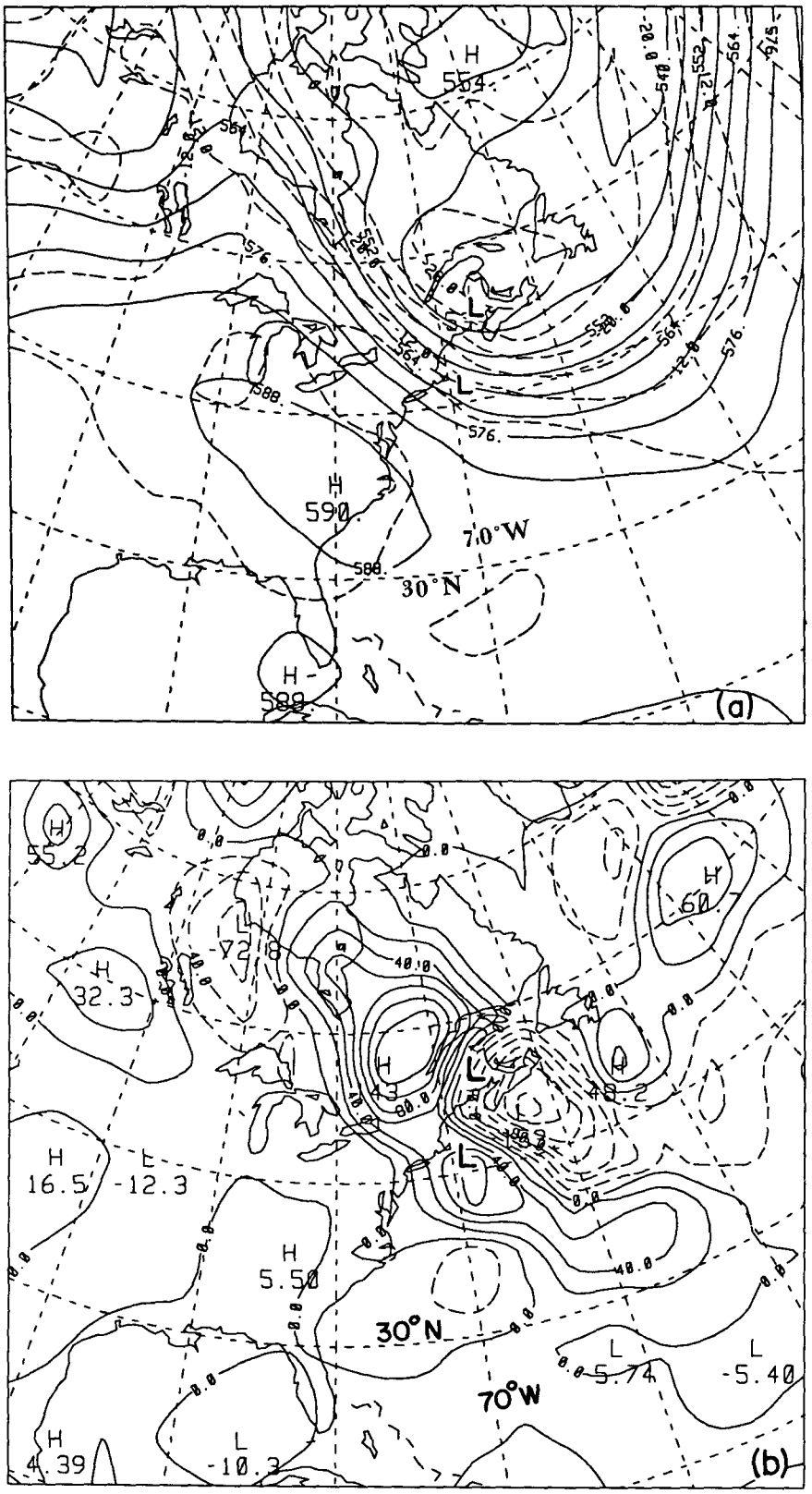

FIG. 10. As for Fig. 4, except for 1200 UTC 9 September 1978.

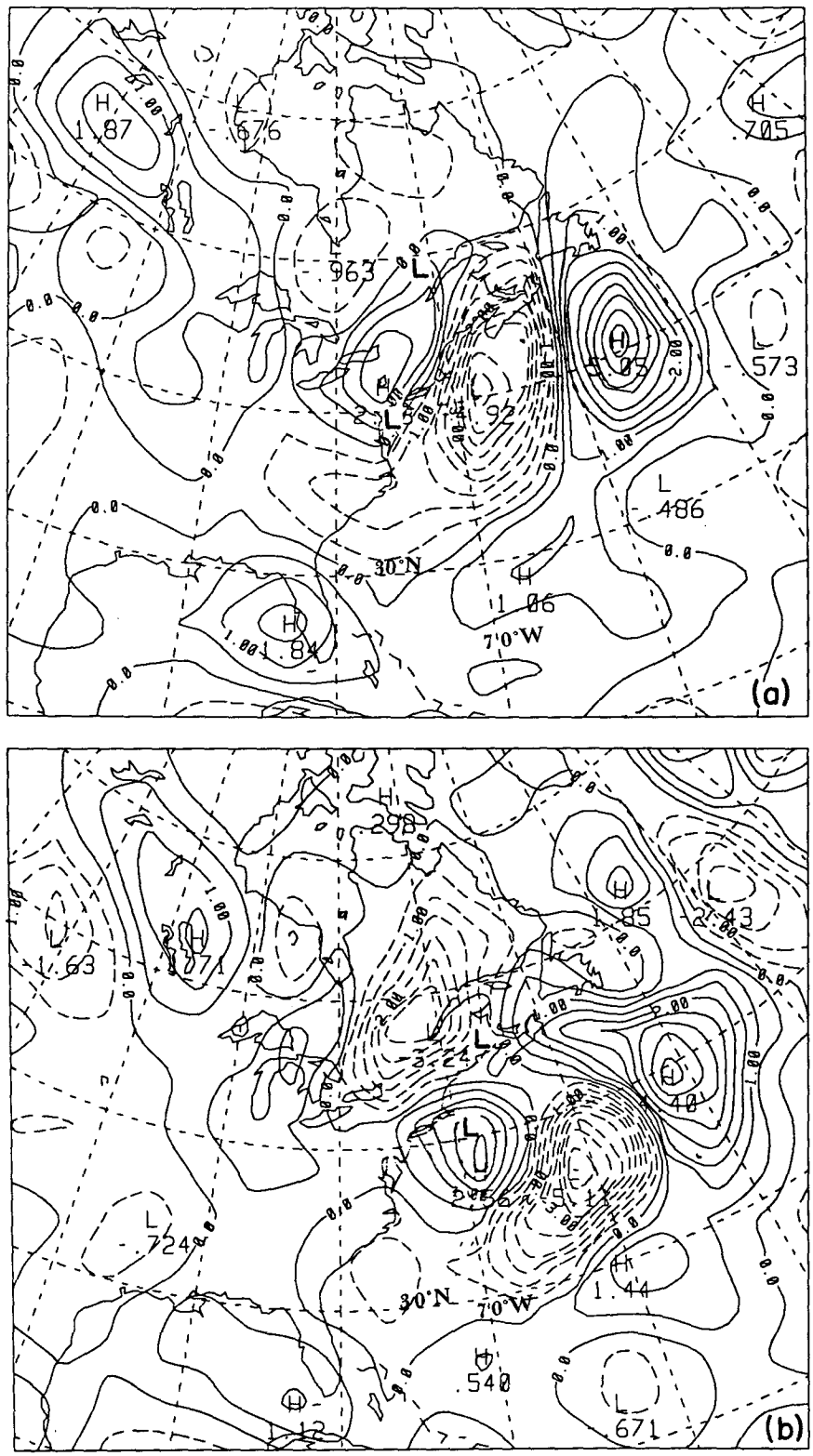

FIG. 11. Absolute geostrophic vorticity advection at 200 mb for (a) 0000 UTC 9 September and (b) 1200 UTC 9 September 1978. Contour interval is 0.5×10^{-9} s^{-2}. The two surface low positions are shown with "L's."

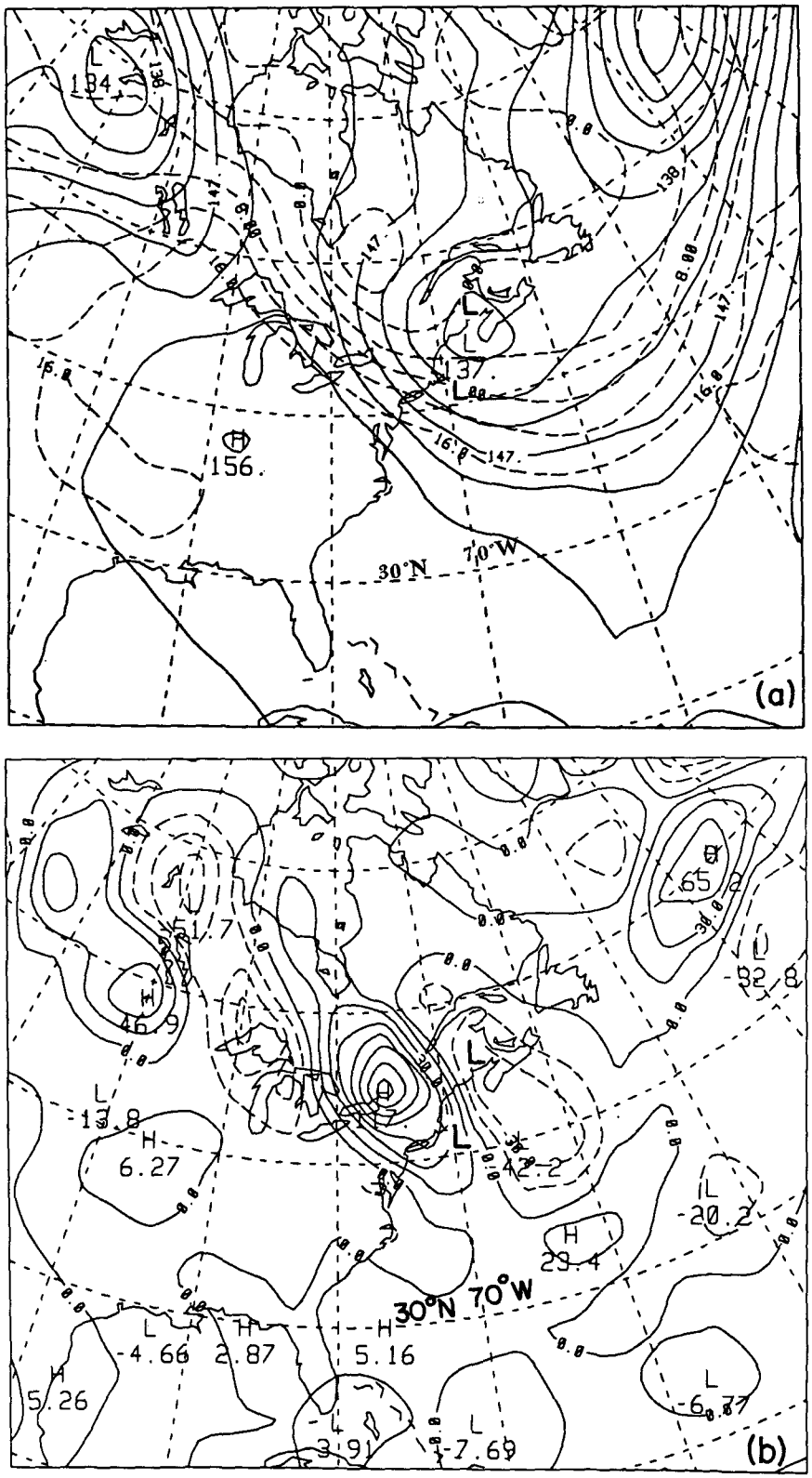

FIG. 12. As for Fig. 5, except for 1200 UTC 9 September 1978.

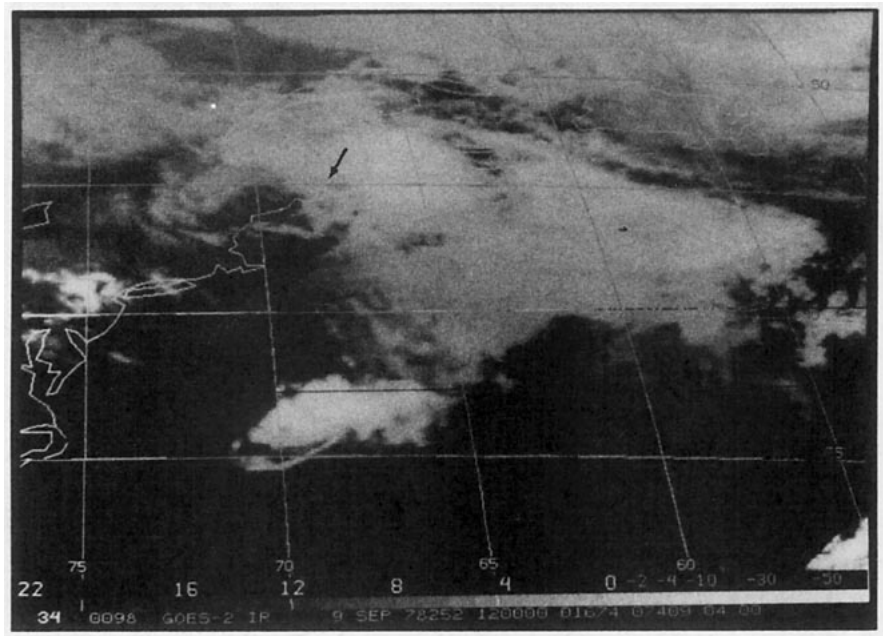

FIG. 13. GOES infrared satellite image for 1200 UTC 9 September 1978 with the same enhancement as for Fig. 6. Arrows point to the positions of surface lows.

throughout Nova Scotia, New Brunswick, and northern New England. These clouds are associated with the deep cyclonic disturbance in eastern Maine, seen in the image as the comma cloud. The separate developing *QE II* cyclone appears as a comma cloud in the image with warm shallow clouds and embedded convective towers along the cold frontal band extending in an arc from 41°N, 69°W around to 36°N, 70°W, consistent with the frontal analysis shown in Fig. 9. The details of the cloud top evolution in this cyclonic system are to be described in the next section.

While it is not possible to document the detailed vertical structure of vertical motions over the *QE II* cyclone at 1200 UTC, we show in Fig. 14 the kinematically computed vertical motions in the Shelburne, Portland, and Caribou triangle (the locations are shown in Fig. 9) that surrounds the northern surface low. The vertical structure of the deep ascent is similar to that seen for the triangle surrounding this low at 0000 UTC (Fig. 8d) in that the ascent peaks near 460 mb and that much of the convergence occurs in the middle troposphere. The deep ascent shown in this triangle is consistent with the strong *Q*-vector convergence seen in this area (Figs. 10b and 12b) and the cold clouds seen within this deep cyclonic system. The substantial upward increase in cyclonic vorticity in this triangle demonstrates this cyclone's cold-core structure that is similar to its vertical vorticity profile seen 12 h earlier (Fig. 8d). The forcing for the *QE II* system to the south appears to be more closely confined to the lower troposphere, even at this onset of maximum explosive intensification. We investigate the mesoscale details of this surface cyclone in section 4.

4. Mesoscale details

Figure 15 shows the detailed 6-h surface analyses of pressure, temperature, and the geostrophic frontogen-

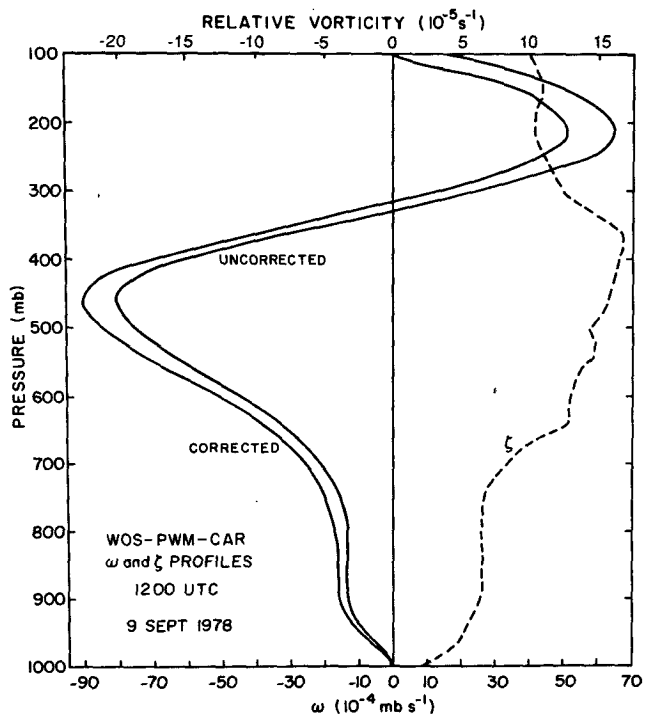

FIG. 14. Vertical profiles of kinematically computed vertical motions (solid, 10^{-4} mb s^{-1}) and vorticity ζ (dashed, 10^{-5} s^{-1}), at 1200 UTC 9 September 1978 for the triangle Shelburne (WOS), Portland (PWM), and Caribou (CAR). Locations of these stations are shown in Fig. 9.

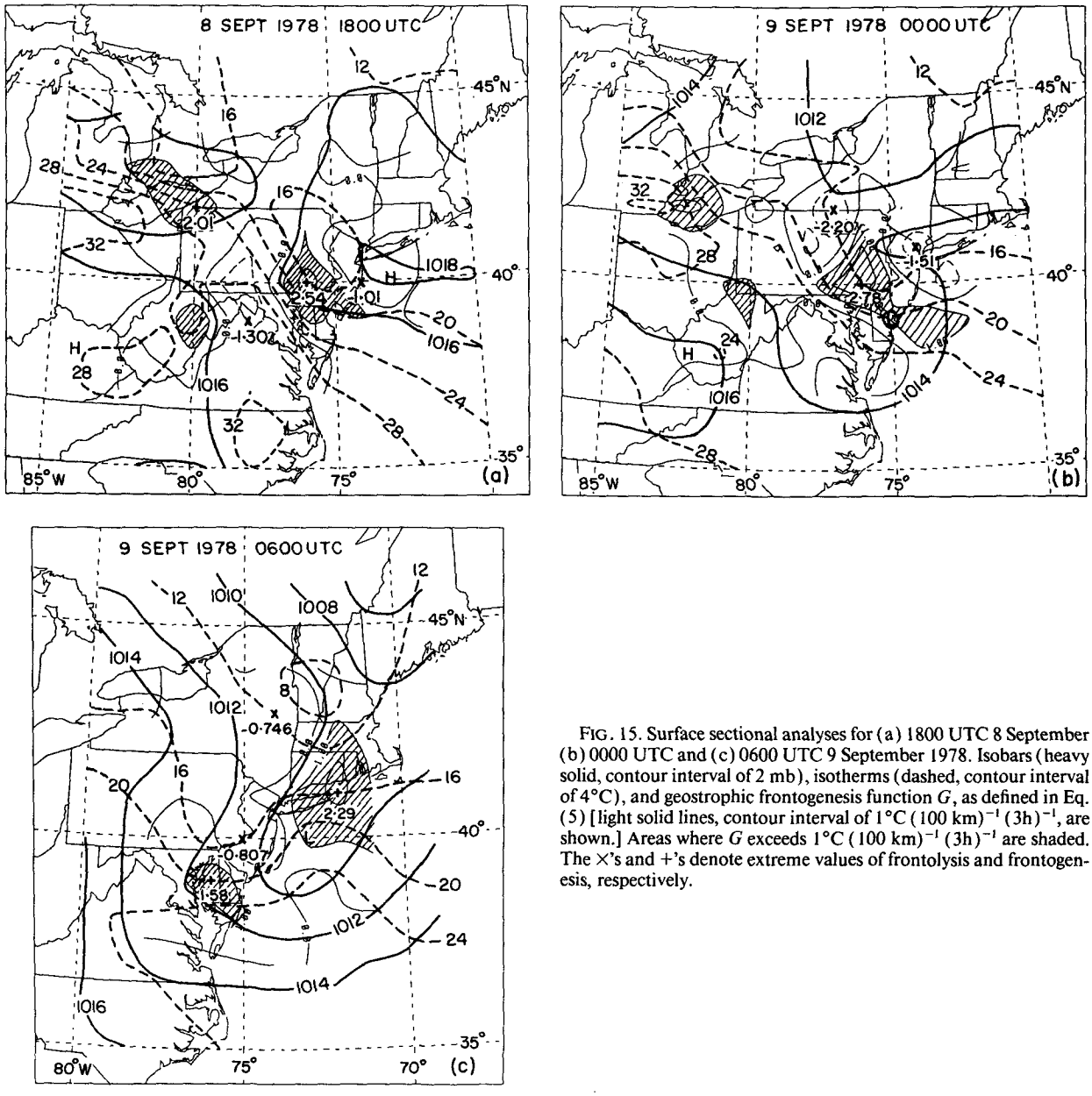

FIG. 15. Surface sectional analyses for (a) 1800 UTC 8 September (b) 0000 UTC and (c) 0600 UTC 9 September 1978. Isobars (heavy solid, contour interval of 2 mb), isotherms (dashed, contour interval of 4°C), and geostrophic frontogenesis function G, as defined in Eq. (5) [light solid lines, contour interval of 1°C (100 km)$^{-1}$ (3h)$^{-1}$, are shown.] Areas where G exceeds 1°C (100 km)$^{-1}$ (3h)$^{-1}$ are shaded. The X's and +'s denote extreme values of frontolysis and frontogenesis, respectively.

esis function G, as defined in Eq. (5), for the 12-h period beginning 1800 UTC 8 September. At 1800 UTC, the area of strong surface baroclinity, extending northwestward from the Delmarva Peninsula to Lake Erie, is situated in a deformation zone between anticyclones located south of Long Island and in Kentucky. Though no closed cyclonic circulation is observed at this time, a region of strong geostrophic frontogenesis exists along this baroclinic zone in southeastern Pennsylvania. The maximum point value, in excess of 2.5°C (100 km)$^{-1}$ (3 h)$^{-1}$, is greater than the comparable antecedent values reported by Gyakum and Barker (1988) for the Southeast States cyclone of 1984. This geostrophic frontogenesis, in the presence of a horizontal gradient of 8°C (100 km)$^{-1}$ implies a geostrophic deformation of approximately 3×10^{-5} s^{-1}. This deformation yields an e-folding time of approximately 9 h. Such a time scale suggests the importance of mesoscale processes in the development of the surface front along which the cyclone subsequently forms.

By 0000 UTC 9 September, a closed cyclonic circulation develops west of Atlantic City along this zone of active frontogenesis. The northwest–southeast orientation of the front is collocated with the deep convective clouds shown in Fig. 6. The analysis, truncated to a 1° latitude–longitude grid, and thus smoothing our manually analyzed central pressure of 1011 to 1012 mb, shows the low in its correct location. The half-

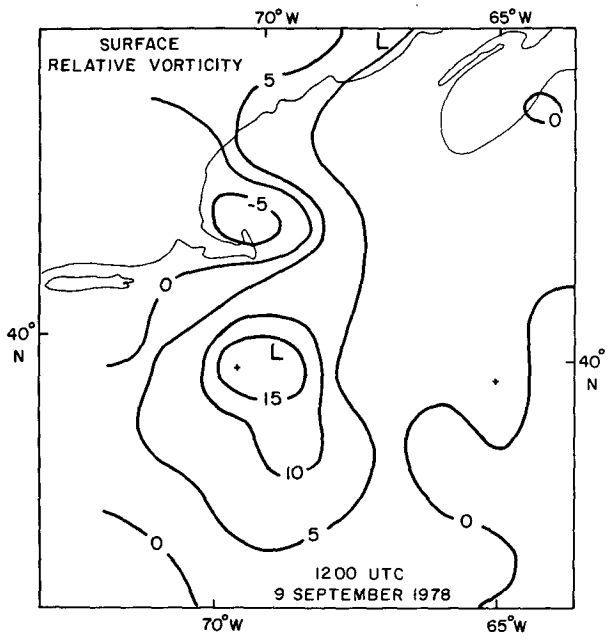

FIG. 16. Surface relative vorticity field for 1200 UTC 9 September 1978. (Units are 10^{-5} s^{-1}.)

wavelength of 450 km, as determined by the average of the distances between the incipient low and the West Virginia and Long Island ridges, also suggests the cyclogenesis to be a mesoscale event.

The deepening 1008-mb low, has propagated eastward at a speed of 9 m s^{-1} to 40°N, 73°W by 0600 UTC 9 September. Additionally, the cyclone shows a more mature pattern of cold air and cold frontogenesis to its south and west, and warm air and warm frontogenesis to its east and north. Such frontogenesis provides an independent verification that cyclogenesis has been occurring, since cold and warm frontal intensification would be expected in response to a developing surface cyclone (Hoskins 1982). Gyakum (1983a) has also shown the surface winds in support of the surface vorticity center's existence prior to this time.

By 1200 UTC, the surface low has deepened to 1004 mb (Fig. 9) and has moved to a position southeast of Cape Cod. Its average propagation speed during the preceding 6 h has increased to 15 m s^{-1}. Gyakum (1983a) has shown the maximum surface winds in this cyclone to be 18 m s^{-1} by this time. The detailed surface vorticity field (Fig. 16) for this time, based upon a 1° latitude–longitude wind analysis and supported by supplementary scatterometer-derived winds (see Fig. 8 of Gyakum 1983a), shows the maximum of 17 $\times 10^{-5}$ s^{-1} to be located over the southern surface low where strong surface baroclinity is prominent. At the same time, the northern cyclone in eastern Maine is also deepening, though its surface winds and vorticity are considerably weaker than the comparable features found in the cyclone to the south.

To understand further the antecedent surface frontogenesis related to this surface cyclogenesis, we present the time series of hourly weather observations on the cold side at Trenton, New Jersey and on the warm side of the front at Dulles Airport (Fig. 17). The stations, located 250 km apart, are each associated with distinct air masses. Dulles, situated in a subtropical air mass, experiences a 2100 UTC temperature of nearly 32°C on 8 September with dewpoints that afternoon as high as 22°C. The strongly heated air at Dulles contrasts sharply with the cool easterly winds and foggy, showery conditions seen at Trenton. The falling or steady surface temperatures at Trenton through the day, combined with the sharp warming at Dulles provide for a 15°C temperature contrast between the stations by 2100 UTC 9 September. The showery and foggy conditions at Trenton are likely associated with a cool stable surface layer lying below a conditionally unstable layer, such as had been reported at JFK airport at 0000 UTC that evening (Fig. 7c). The surface cyclogenesis had occurred by 0000 UTC in a hyperbaroclinic zone of active surface frontogenesis. Gyakum and Barker (1988) have also shown a subsynoptic-scale cyclone to have developed in a surface frontogenetic region associated with both geostrophic deformation and with differential surface diabatic heating.

Additional infrared-enhanced satellite images for 9 September 1978 (Fig. 18) shown every 3 h, help to document the processes associated with the *QE II* cyclone's incipient development. This satellite sequence, in combination with the earlier presentation, is designed to illustrate the evolution of the *QE II* cyclone from a shallow mesoscale wave developing along a region of active surface frontogenesis in New Jersey to a synoptic-scale system in which there was a clear interaction with the 500-mb vorticity maximum whose origin can be traced back to the Canadian Northwest Territories.

At 0000 UTC, the frontal cyclone is seen as the area of cold convective cloud in New Jersey (Figs. 3 and 6). Additional convective cells extend west and north along the line of surface frontogenesis. The surface low in eastern Quebec is seen as a circulation center embedded within the northern cloud mass at approximately 49.0°N, 71.0°W. A more detailed view of the New Jersey low (Fig. 18a) shows it to exist on the western edge of the deep convective system. The buoy report (40.1°N, 73.0°W), 140 km northeast of the low and south of Long Island, of a southeast wind at 8 m s^{-1} at 0000 UTC (Fig. 18a) is consistent with our analysis of the developing surface circulation (Fig. 15). By 0300 UTC (Fig. 18b), the surface low is located at approximately 40.0°N, 73.8°W; the deep convection is moving southeastward, and the cloud top temperatures directly over the surface low are about 0°C (700 mb). The offshore surface winds help to define the surface vortex, while both JFK and Islip on the southern part of Long Island were reporting easterly winds. By 0600

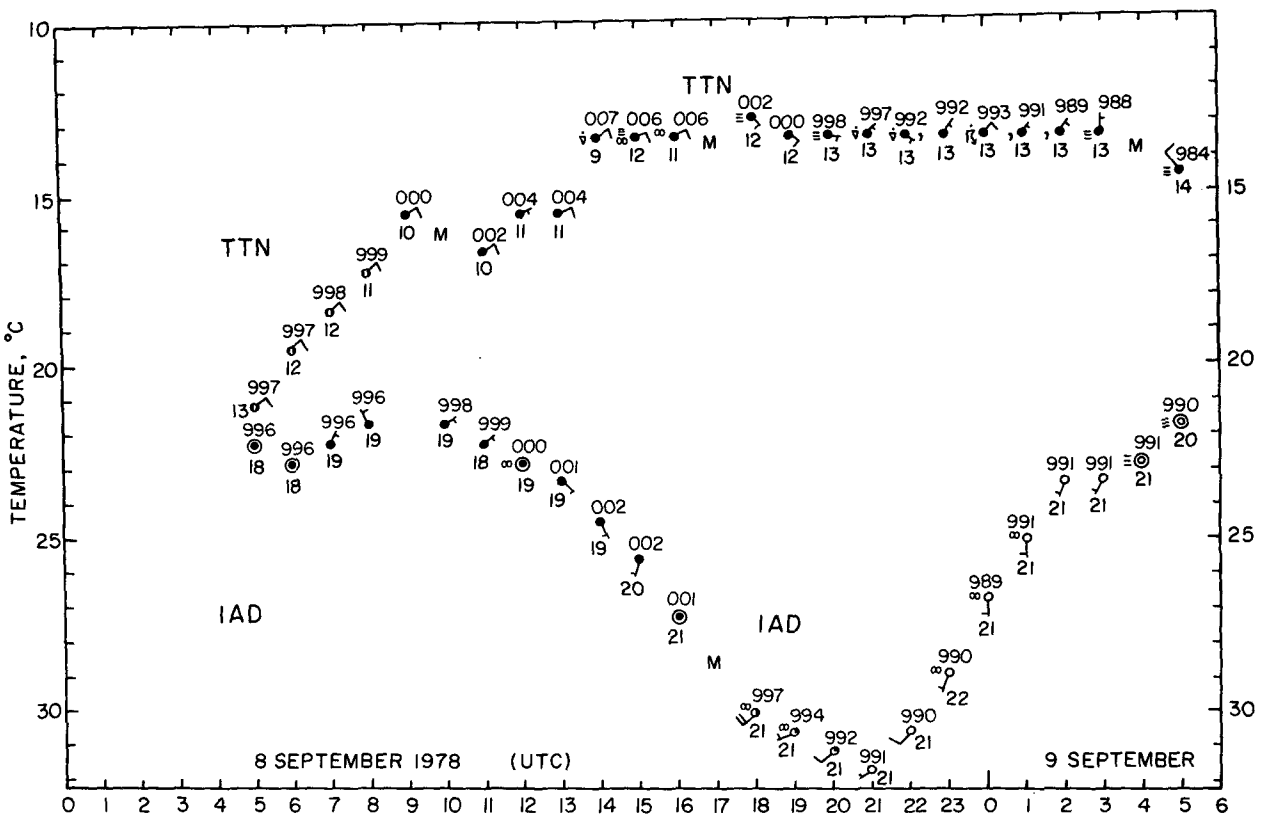

FIG. 17. Time series of hourly observations at Trenton (TTN) and Dulles International airports (IAD) from 0500 UTC 8 September through 0500 UTC 9 September 1978. Stations are plotted according to their temperature (ordinate, °C). Dewpoint (°C), winds (plotted as in Fig. 7), cloud amount and weather are plotted conventionally. A missing observation is indicated as an "M." Station locations are shown in Fig. 3.

UTC (Figs. 18c,d), the 1008-mb low is just to the north-northwest of the buoy at 40.1°N, 73.0°W. The associated cold front band of shallow cloud elements has penetrated to the extreme northwest edge of the large cold cloud (convective) complex seen to the southeast of the low. The low's associated cloudiness through eastern Long Island and southern New England is evidently related to the warm frontogenesis (Fig. 15c) in this region. The northern low is located at approximately 47.5°N, 70.0°W. The mesoscale view at 0600 UTC (Fig. 18d) shows the developing low to be well separated from the southeastward moving convective region. This particular region, though initially associated with the incipient cyclone, translated with the strong upper-tropospheric northwesterly flow (see Fig. 7). The shallow surface low was apparently steered by the lower-tropospheric westerlies. The cloud tops in the vicinity of the low are approximately 18°C or at about 950 mb. By 0900 UTC (Fig. 18e), the low at 40.3°N, 71.2°W has cloud tops of approximately 15°C or 900 mb directly over it. The cold frontal band extends southwestward from the center with deepening convective cloud clusters of 8°C or 650–700 mb tops that are approaching the northwest edge of the large convective complex. At 1200 UTC (Figs. 13 and 18g), a well-defined cold frontal band extends from the low at 40.5°N, 69.5°W. The circulations around both the *QE II* low to the south, with its cold frontal clouds casting shadows along the northwest side of the convective complex, and the Maine low (45.5°N, 68.0°W) are well documented in the morning visible image at 1130 UTC (Fig. 18f). Though the low's central pressure is 1004 mb and the surface relative vorticity is 17 $\times 10^{-5}$ s^{-1}, its cloud tops are still warm (11°C) and shallow (about 800 mb). This observation is consistent with our large-scale analysis (Fig. 10) for this region, suggesting ascent in the lower troposphere and descent in the middle troposphere.

The subsequent images show clearly the evolution of the southern cyclone into the dominant system. At 1500 UTC (Fig. 18h), the low has moved to approximately 40.5°N, 66.5°W. The convective elements are lined up along the cold frontal band that extends southwestward to 37.0°N, 68.0°W. The cloud structure appears similar to the "head" configuration described by Böttger et al. (1975) as being unique to explosively developing marine cyclones. The northern system has moved offshore to a position west of Yarmouth at

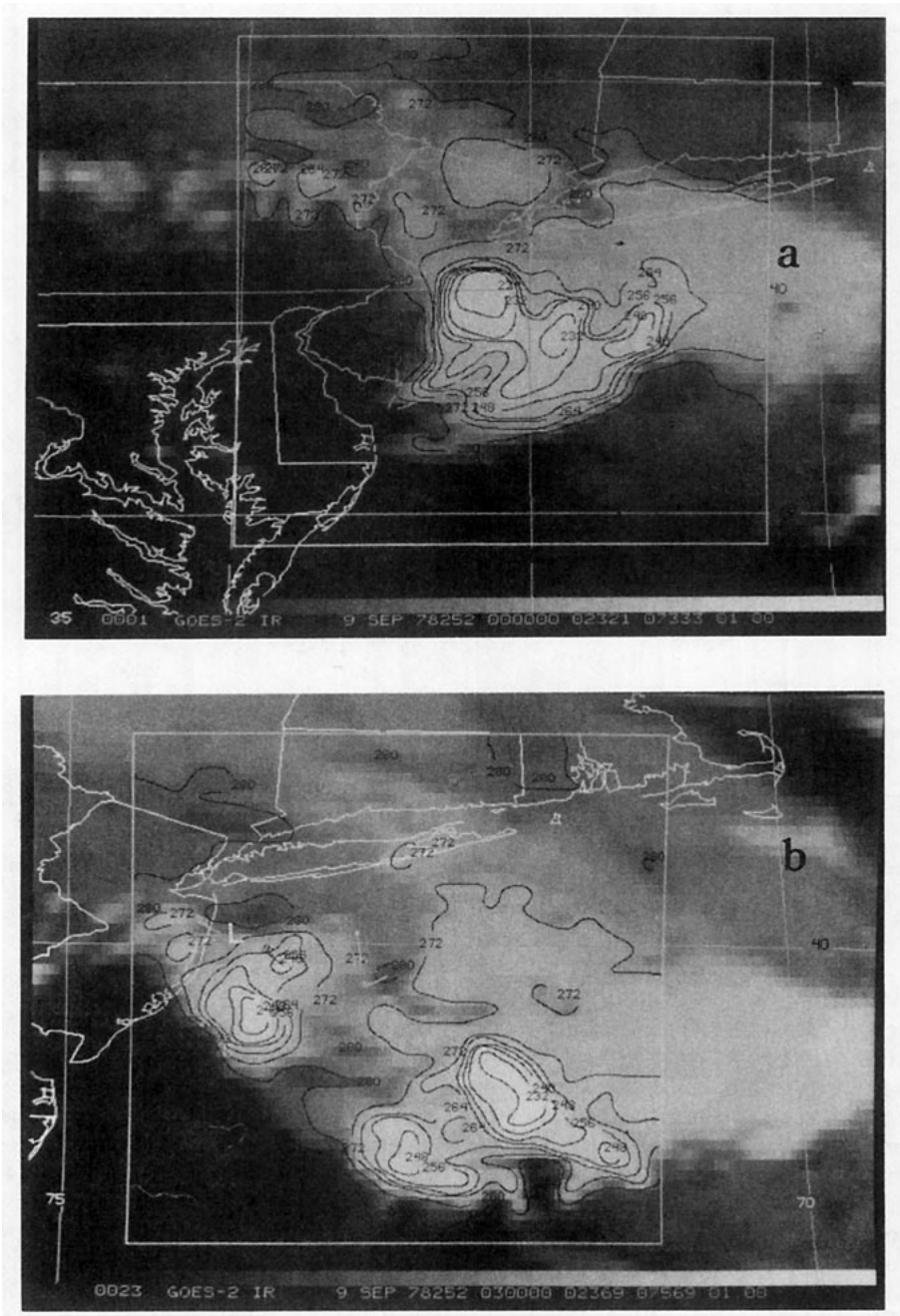

FIG. 18. Geostationary satellite images derived from McIDAS system for 9 September 1978. Infrared (IR) enhancement temperatures (°C) are shown at the bottom of the appropriate images. Mesoscale infrared enhancements show isotherms of cloud top temperatures (K) and the surface low position (indicated with an "L"). Selected surface buoy and ship winds are shown by small squares at the station with other cloud-track winds also shown; the plotting convention is found in Fig. 7. Arrows point to the position of the low center in the images of the larger regions. (a) Mesoscale IR at 0000 UTC, (b) mesoscale IR at 0300 UTC, (c) IR for 0600 UTC. The *QE II* cyclone is approximately collocated with the buoy (see the white dot) at 40.1°N, 73.0°W south of Long Island, (d) mesoscale IR at 0600 UTC, (e) mesoscale IR at 0900 UTC, (f) visible at 1130 UTC, (g) mesoscale IR at 1200 UTC, (h) IR at 1500 UTC, (i) IR at 1800 UTC, (j) IR at 2100 UTC.

43.5°N, 67.0°W. By 1800 UTC (Fig. 18i), the southern low has moved to 40.2°N, 63.0°W. Its associated convective towers have continued to develop along the frontal band and the system's meridional growth continues. The surface system to the south of Nova Scotia at 43.0°N, 66.0°W is weakening and losing its identity

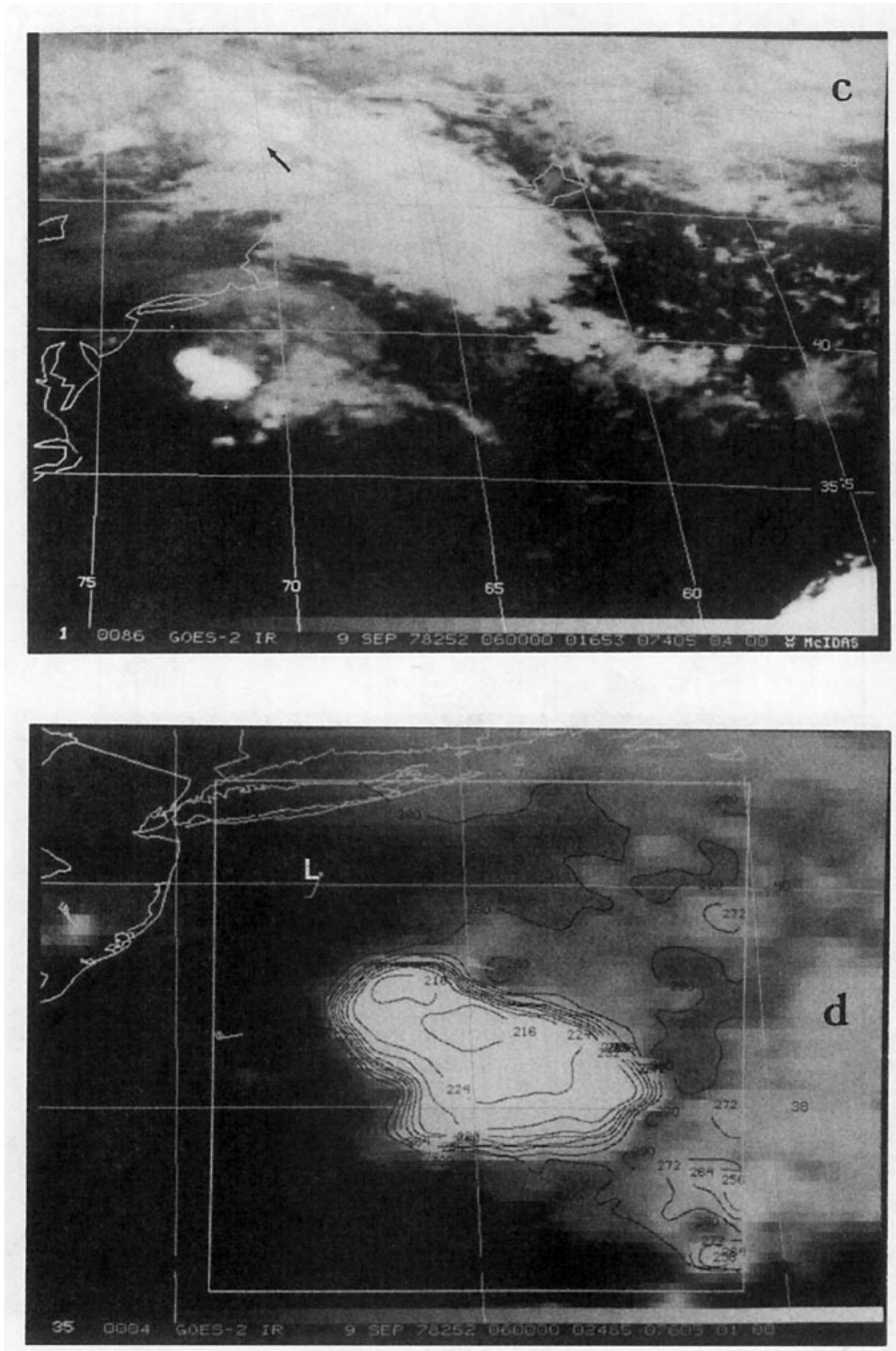

FIG. 18. (*Continued*)

in the presence of the strong cold advection of the *QE II* storm. At 2100 UTC (Fig. 18j), the *QE II* cyclone at 40.3°N, 60.0°W has all of the classic signatures of an intense extratropical system with its warm frontal bands extending to 46.0°N, and its cold frontal band having triggered or interacted with convective systems to its southwest. The northern cyclone has nearly lost its identity in the expanding region of cold advection in the wake of the primary system.

5. Concluding discussion

We have documented the evolution of the explosively developing *QE II* storm in terms of a two-stage process. The first stage consists of the 12-h period beginning at 0000 UTC 9 September 1978, during which the cyclone deepens 7 mb. Much of the previous observational and modeling research into this case has focused upon the subsequent 24-h period (1200 UTC

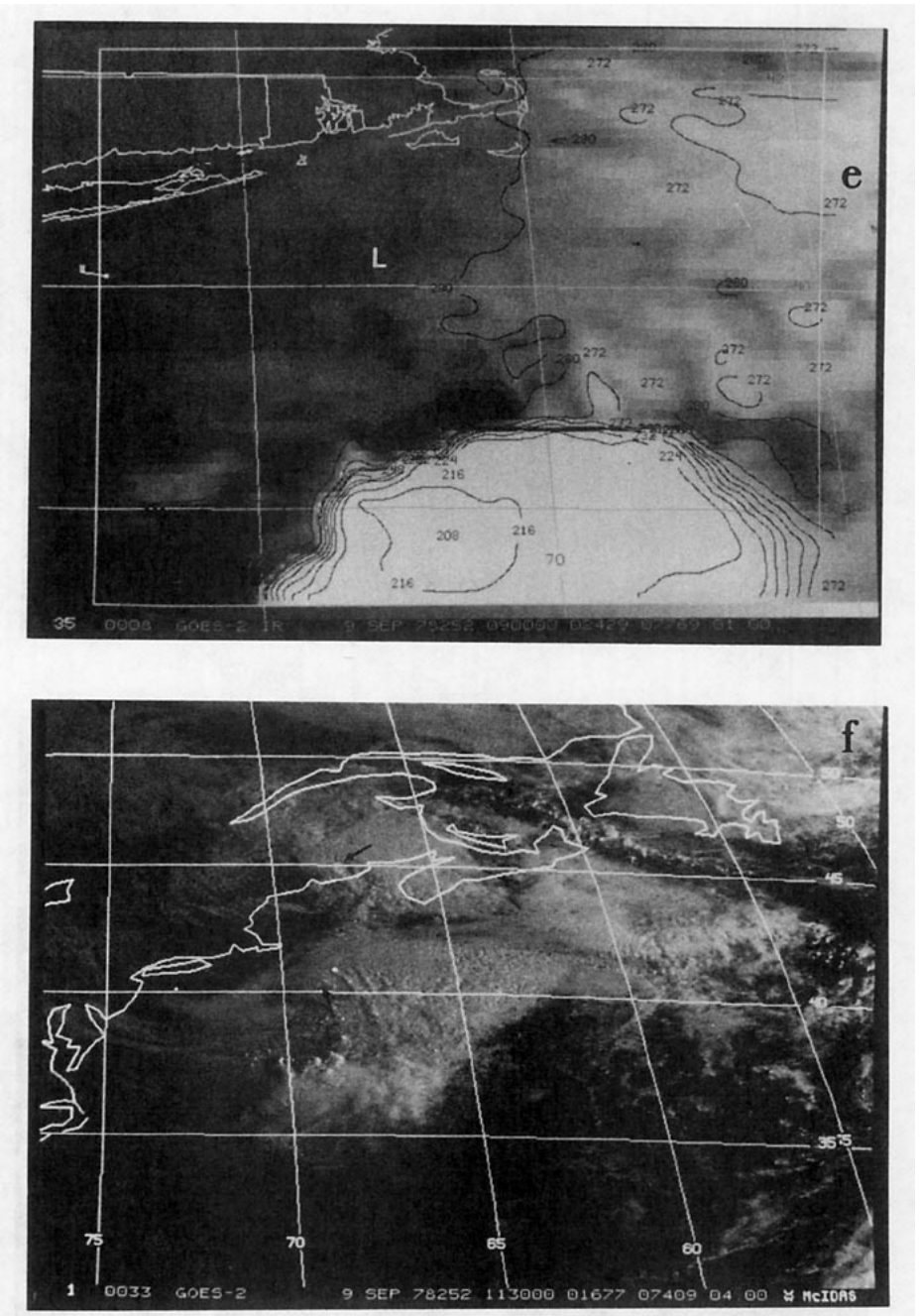

FIG. 18. (*Continued*)

9 September through 1200 UTC 10 September) of extraordinary 60-mb central pressure fall. We define this particular time period as the second stage of the cyclogenesis. During this period the cyclone deepened to 945 mb, and the system contained hurricane-force winds (Gyakum 1983a).

The focus of this work has been the physical description of the first stage of this cyclogenesis process. We regard this particular stage of development, though it lasts for only 12 h, as being especially crucial to the following 24-h period of explosive deepening. During this first stage, the surface cyclone formed and developed until its winds strengthened to 18 m s^{-1} and its geostrophic vorticity increased to 30×10^{-5} s^{-1}. Such a large vorticity may have enhanced the cyclone intensification during the subsequent period of explosive deepening (stage II). Such an enhancement is suggested by our discussion of the vorticity equation (2) in which

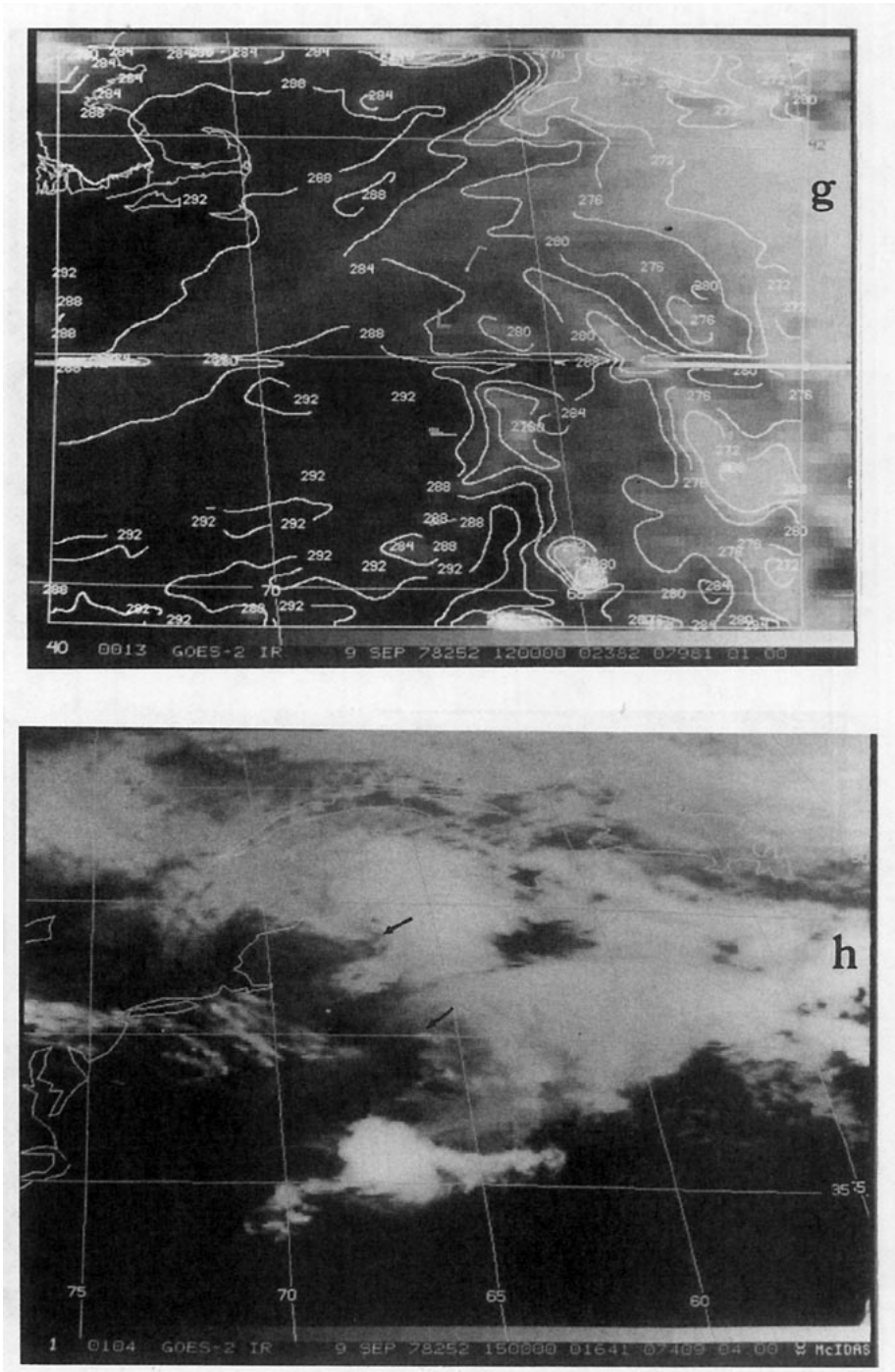

FIG. 18. (*Continued*)

the rate of vorticity increase at the cyclone center associated with convergence is directly proportional to the vorticity itself.

What has not been discussed in the literature is the fact that the preexisting upper-tropospheric cyclonic disturbance was actively associated with another, distinct and deepening, surface cyclone whose path during the *QE II* cyclone's stage I period (0000–1200 UTC 9 September) extended from central Quebec to eastern Maine.

We have documented the dynamical structures of each surface cyclone as being fundamentally different during this 12-h time period. The northern system is shown to be a deep tropospheric cold-core disturbance

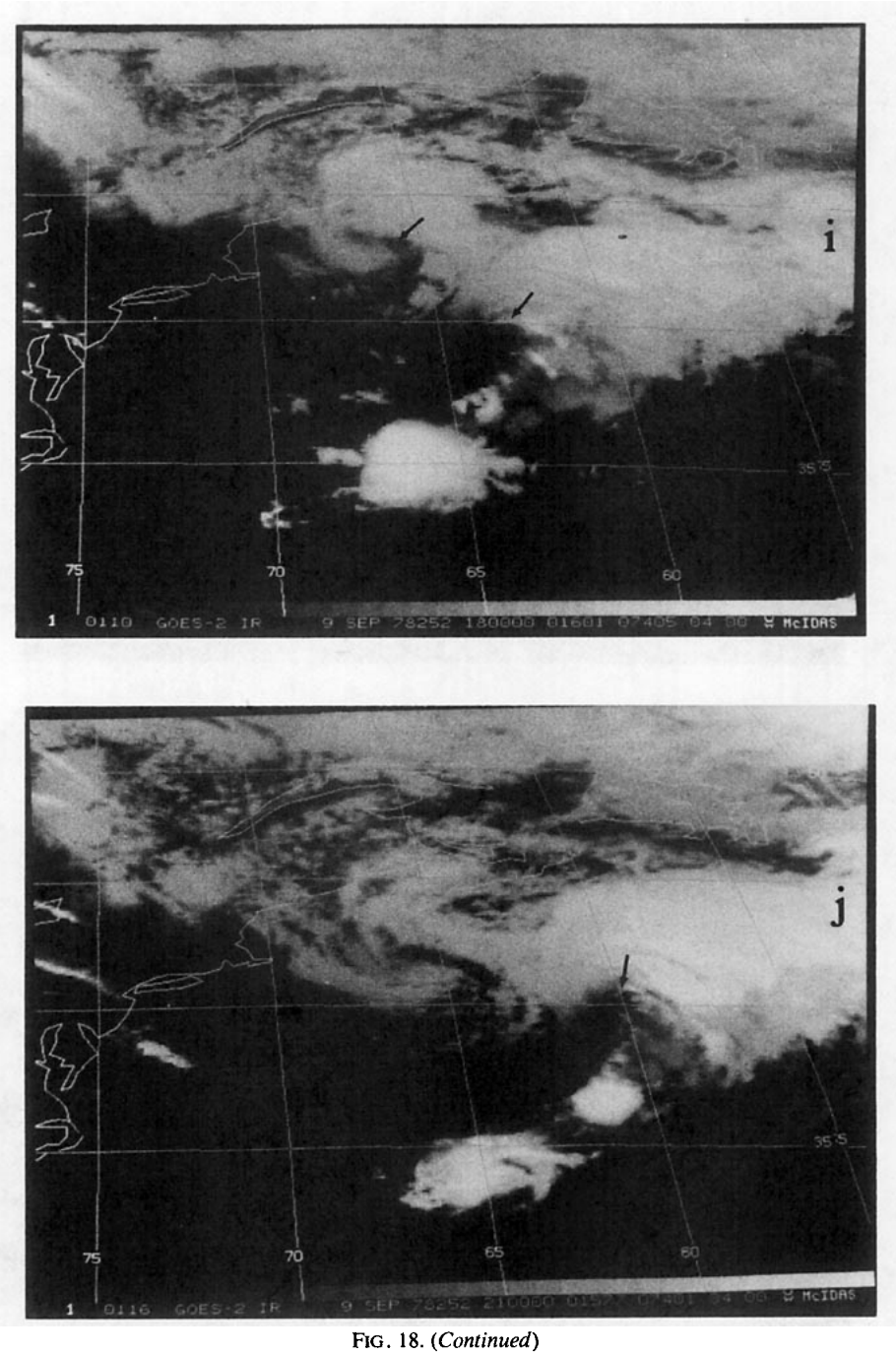

FIG. 18. (*Continued*)

that continues to intensify in the absence of any active surface front. Rather, its deepening occurs in the presence of a broad horizontal temperature gradient, a baroclinic process introduced many years ago by Charney (1947) and Eady (1949). More recent work by Farrell (1984) suggests that middle-latitude cyclogenesis may often be described in terms of a finite amplitude upper-level disturbance inducing a low-level disturbance, a process described in terms of isentropic potential vorticity by Hoskins et al. (1985). This particular process appears to apply to the northern low, since the strong 500-mb trough could be traced back in time to 1200 UTC 7 September (Fig. 2). The incipient *QE II* cyclone, on the other hand, is shown to be a shallow, warm-core disturbance during its first 12 h of development. Its formation occurs along a preex-

isting deformation zone of strong geostrophic frontogenesis between two surface anticyclones. The surface heating gradient across this front also contributed to the frontogenesis process. Kuo et al. (1991b) have shown from their modeling work, that surface heat fluxes can contribute positively to frontogenesis and the associated surface vorticity increase during the early stages of a cyclone's development. The *QE II* cyclone intensified during its first 12 h of existence apparently without any support from the 500-mb vorticity maximum.

We have traced the eastward movement of this frontal cyclone throughout this first stage of development with the aid of detailed surface ship and buoy observations and satellite imagery. Though the system developed along a preexisting active front, the system's circulation begins to form its own warm and cold frontogenesis regions only 6 h after its onset. Throughout this first stage of development cloud tops along these developing fronts are no higher than 800 mb, corroborating our diagnostic calculations of the disturbance's shallow structure.

By 1200 UTC 9 September, the onset of stage II of the cyclogenesis, the *QE II* cyclone still had cloud tops reaching only to 800 mb. The separate and deep cold-core surface cyclone was still extant in eastern Maine at this time, and in a favorable downstream position with respect to the 500-mb vorticity maximum. This information, along with the independent gridpoint diagnoses showing middle-tropospheric subsidence over the *QE II* cyclone at this time, leads us to conclude it is still a shallow system at this time.

Upon commencement of the stage II cyclone intensification, however, the *QE II* cyclone continues to accelerate eastward, deepen and expand horizontally and vertically. Early in this 24-h time period, we observe the original northern cold-core cyclone to simply lose its identity in the midst of the expanding region of strong cold advection behind the *QE II* cyclone. Sometime during the first 12 h of this stage II intensification, the upper-tropospheric trough was responsible for accelerating the cyclone intensification rate to well beyond the threshold "bomb" criterion. In addition to the fact that convection was observed near the center of the low (see Figs. 18i, j) and the environmental lapse rates were nearly moist adiabatic, indicating an especially strong response to the approaching upper-tropospheric trough, we suggest that the stage I intensification may have played a significant role in enhancing the later stage II surface cyclone intensification. This so-called "antecedent" intensification, that amplifies the surface response to a given amount of upper-level forcing (associated with a given amount of surface convergence), may be another crucial physical process that distinguishes explosively developing cyclones from the more benign set of cases. As an example, in spite of smoothing the details of the sea-level pressure and wind fields at 1200 UTC 9 September, Kuo et al. (1991a) still achieved a realistic-appearing simulation of the *QE II* storm later during its explosive intensification. However, the modeled 967-mb central pressure was still substantially above the observed value of 945 mb (Gyakum 1983a). It is possible that a more realistic wind and pressure analysis at 1200 UTC 9 September, or a forecast from an earlier time, would have provided a better forecast of the cyclone's ultimate strength.

Our work suggests that the explosive intensification of the *QE II* storm may be understood in terms of an interaction of two separate vorticity maxima—one moving southeastward in the upper troposphere from the Northwest Territories of Canada, and the other disturbance originating along a zone of strong surface frontogenesis to the west of Atlantic City. These disturbances, each of substantial intensity and each of different origin, interacted explosively offshore in the western Atlantic Ocean after 1200 UTC 9 September. Such an interaction of two cyclonic disturbances appears similar to the extratropical cyclogenesis depiction of Bleck (1990). The importance of this interaction from an isentropic potential vorticity (IPV) perspective (Hoskins et al. 1985) is that two induced wind fields can act in a cooperative manner to explosively amplify each of the lower and upper IPV anomalies. DiMego and Bosart (1982) have described similar physical conditions in which Tropical Storm Agnes was transformed into an extratropical system. The authors suggest that the vorticity-rich surface boundary layer enhanced its redevelopment when it became associated with cyclonic vorticity advection aloft. Such a synergistic interaction has been shown by Whitaker et al. (1988) to have occurred during the explosive development phase of the Presidents' Day cyclone of 1979. The particularly strong surface cyclonic vortices (positive IPV anomalies) in these cases may have been at least partially generated by diabatic heating associated with the observed cumulus convection.

It is important to reconcile our results with recent research regarding fundamental characteristics of the explosively developing cyclone. Sanders (1986), in studying a set of surface lows in the western Atlantic, finds these cases to be associated with preexisting middle-tropospheric cyclonic disturbances. He also finds that the explosive intensification generally increases with the strength of the upper-level disturbance. Therefore, he describes the process of explosive cyclogenesis in terms of a Petterssen type "B" development (see Petterssen and Smebye 1971) in which a preexisting 500-mb vorticity maximum is the dominant forcing for cyclogenesis. However, all of the time periods studied by Sanders (1986) corresponded to the 24-h period of maximum deepening. Therefore, all of these periods would correspond to the stage II intensification studied in this paper. Additionally, there were

cases in which, though a 500-mb vorticity maximum was clearly extant, its interaction with the particular surface cyclone was not always obvious. The stage I development of the *QE II* cyclone was apparently disassociated from the 500-mb trough that did subsequently interact with the cyclone during stage II. However, this trough, extant during stage I, was associated with another distinct surface disturbance to the north. Other cases of explosive cyclogenesis in the western Atlantic may preferentially follow similar patterns.

The suggestion of finite-amplitude upper and lower cyclonic disturbances developing independently of one another and subsequently interacting explosively provides us with a physical justification for stratifying the development of a "bomb" into two stages. Indeed, the Presidents' Day cyclone of 18–19 February 1979 has been shown by the analyses of Bosart (1981), Bosart and Lin (1984), Uccellini et al. (1984, 1985) and Uccellini et al. (1987) to have consisted of a similar two-stage process. The surface cyclone formed in a region of active coastal frontogenesis and its associated shallow thermally direct circulation during stage I; its mature vortex subsequently interacted with a strong polar trough traveling eastward from the North American continent. This interaction constituted the second stage of the cyclone's life cycle during which its explosive intensification occurred.

The formation of this cyclone and others along preexisting zones of strong frontogenesis provides motivation to study incipient "bomb" development in such regions. Short and shallow frontal waves have been studied throughout this century since the Norwegians began to document the frontal cyclone. Eliassen (1965) has presented a thorough review of the research into the frontogenesis and cyclogenesis processes. Frontal waves have been documented, more recently, both observationally (Keshishian and Bosart 1987) and theoretically (Sinton and Mechoso 1984; Moore and Peltier 1987). It is possible that rapidly developing cyclones preferentially form as a consequence of an instability along intensifying hyperbaroclinic zones. The finding of Sanders and Gyakum (1980) that explosive cyclone intensification is often located near zones of strong sea surface temperature gradients is consistent with such a possibility.

We suggest that further diagnostic modeling studies be performed, upon cases such as this, that focus upon the surface cyclone's complete life cycle that includes all stages of its deepening. It is possible that the particular stage I intensification documented in this study may be a crucial precursor to the subsequent explosive intensification process. Especially rapid, cyclone deepening may be due, in part, to a surface cyclone's especially strong intensity at the beginning of this especially rapid deepening period.

Acknowledgments. This work has been supported by the National Science Foundation under Grants ATM-8516263 and ATM-8814816, the Atmospheric Environment Service of Canada, and the Canadian Natural Sciences and Engineering Research Council under operating Grant P0037433. The technical assistance of the University of Wisconsin's Space Science and Engineering Center staff in accessing the satellite imagery is appreciated. The author appreciates the constructive comments of Drs. Lance Bosart, Ying-Hwa Kuo, Wendell Nuss, Richard Reed, Frederick Sanders, Louis Uccellini, De-Lin Zhang and two anonymous reviewers. Mr. Tim Bullock assisted in computing. The drafting expertise of Ms. Ursula Seidenfuss in figure preparation is acknowledged.

REFERENCES

Anthes, R. A., Y.-H. Kuo and J. R. Gyakum, 1983: Numerical simulations of a case of explosive marine cyclogenesis. *Mon. Wea. Rev.*, **111**, 1174–1188.

Bellamy, J. C., 1949: Objective calculations of divergence, vertical velocity and vorticity. *Bull. Amer. Meteor. Soc.*, **30**, 45–49.

Bleck, R., 1990: Depiction of upper/lower vortex interaction associated with extratropical cyclogenesis. *Mon. Wea. Rev.*, **118**, 573–585.

Bosart, L. F., 1981: The Presidents' Day snowstorm of 18–19 February 1979: A subsynoptic-scale event. *Mon. Wea. Rev.*, **109**, 1542–1566.

——, and F. Sanders, 1981: The Johnstown flood of July 1977: A long-lived convective system. *J. Atmos. Sci.*, **38**, 1616–1642.

——, and S. C. Lin, 1984: A diagnostic analysis of the Presidents' Day storm of February 1979. *Mon. Wea. Rev.*, **112**, 2148–2177.

Böttger, H., M. Eckardt and U. Katergiannakis, 1975: Forecasting extratropical storms with hurricane intensity using satellite information. *J. Appl. Meteor.*, **14**, 1259–1265.

Charney, J. G., 1947: The dynamics of long waves in a baroclinic westerly current. *J. Meteor.*, **4**, 135–162.

DiMego, G. J., and L. F. Bosart, 1982: The transformation of tropical storm Agnes into an extratropical cyclone. Part II: Moisture, vorticity and kinetic energy budgets. *Mon. Wea. Rev.*, **110**, 412–433.

Eady, E. T., 1949: Long waves and cyclone waves. *Tellus*, **1**, 33–52.

Eliassen, A., 1965: Motions of intermediate scale: Fronts and cyclones. *Advances in Earth Science. Contributions to the International Conference on the Earth Sciences*, P. M. Hurley, ed., 111–138.

Emanuel, K. A., 1983: On assessing local conditional symmetric instability from atmospheric soundings. *Mon. Wea. Rev.*, **111**, 2016–2033.

——, 1988: Observational evidence of slantwise convective adjustment. *Mon. Wea. Rev.*, **116**, 1805–1816.

Farrell, B., 1984: Modal and nonmodal baroclinic waves. *J. Atmos. Sci.*, **41**, 668–673.

Gyakum, J. R., 1983a: On the evolution of the *QE II* storm. Part I: Synoptic aspects. *Mon. Wea. Rev.*, **111**, 1137–1155.

——, 1983b: On the evolution of the *QE II* storm. Part II: Dynamic and thermodynamic structure. *Mon. Wea. Rev.*, **111**, 1156–1173.

——, and E. S. Barker, 1988: A case study of explosive subsynoptic-scale cyclogenesis. *Mon. Wea. Rev.*, **116**, 2225–2253.

——, J. R. Anderson, R. H. Grumm and E. L. Gruner, 1989: North Pacific cold-season surface cyclone activity: 1975–1983. *Mon. Wea. Rev.*, **117**, 1141–1155.

Hadlock, R., and C. W. Kreitzberg, 1988: The Experiment on Rapidly Intensifying Cyclones over the Atlantic (ERICA) field study: Objectives and plans. *Bull. Amer. Meteor. Soc.*, **69**, 1309–1320.

Hoskins, B. J., 1982: The mathematical theory of frontogenesis. *Ann. Rev. Fluid Mechan.*, **14**, 131–151.

——, and M. A. Pedder, 1980: The diagnosis of midlatitude synoptic development. *Quart. J. Roy. Meteor. Soc.*, **106**, 707–719.

——, I. Draghici and H. C. Davies, 1978: A new look at the omega-equation. *Quart. J. Roy. Meteor. Soc.*, **104,** 31–38.

——, M. E. McIntyre and A. W. Robertson, 1985: On the use and significance of isentropic potential vorticity maps. *Quart. J. Roy. Meteor. Soc.*, **111,** 877–946.

Keshishian, L. G., and L. F. Bosart, 1987: A case study of extended East Coast frontogenesis. *Mon. Wea. Rev.*, **115,** 100–117.

Kuo, Y.-H., M. A. Shapiro and E. G. Donall, 1991a: The interaction of baroclinic and diabatic processes in a numerical simulation of a rapidly intensifying extratropical marine cyclone. *Mon. Wea. Rev.*, **119,** 368–384.

——, R. J. Reed and S. Low-Nam, 1991b: Effects of surface energy fluxes during the early development and rapid intensification stages of winter cyclones in the western Atlantic. *Mon. Wea. Rev.*, **119,** 457–476.

Mass, C. F., H. J. Edmon, H. J. Friedman, N. R. Chaney and E. E. Recker, 1987: The use of compact discs for the storage of large meteorological and oceanographic data sets. *Bull. Am. Meteor. Soc.*, **68,** 1556–1558.

Moore, G. W. K., and W. R. Peltier, 1987: Cyclogenesis in frontal zones. *J. Atmos. Sci.*, **44,** 384–409.

O'Brien, J. J., 1970: Alternative solutions to the classical vertical velocity problem. *J. Appl. Meteor.*, **9,** 197–203.

Palmén, E., and C. W. Newton, 1969: *Atmospheric Circulation Systems: Their structure and physical interpretation.* Academic Press, 603 pp.

Petterssen, S., and S. Smebye, 1971: On the development of extratropical cyclones. *Quart. J. Roy. Meteor. Soc.*, **97,** 457–485.

Reed, R. J., and M. D. Albright, 1986: A case study of explosive cyclogenesis in the eastern Pacific. *Mon. Wea. Rev.*, **114,** 2297–2319.

Roebber, P. J., 1984: Statistical analysis and updated climatology of explosive cyclones. *Mon. Wea. Rev.*, **112,** 1577–1589.

Rogers, E., and L. F. Bosart, 1986: An investigation of explosively deepening oceanic cyclones. *Mon. Wea. Rev.*, **114,** 702–718.

Sanders, F., 1986: Explosive cyclogenesis in the west-central North Atlantic Ocean, 1981–84. Part I: Composite structure and mean behavior. *Mon. Wea. Rev.*, **114,** 1781–1794.

——, 1988: Life history of mobile troughs in the upper westerlies. *Mon. Wea. Rev.*, **116,** 2629–2648.

——, and J. R. Gyakum, 1980: Synoptic–dynamic climatology of the "bomb." *Mon. Wea. Rev.*, **108,** 1589–1606.

Sinton, D. M., and C. R. Mechoso, 1984: Nonlinear evolution of frontal waves. *J. Atmos. Sci.*, **41,** 3501–3517.

Tracton, M. S., 1973: The role of cumulus convection in the development of extratropical cyclones. *Mon. Wea. Rev.*, **101,** 573–593.

Uccellini, L. W., 1986: The possible influence of upstream upper-level baroclinic processes on the development of the *QE II* storm. *Mon. Wea. Rev.*, **114,** 1019–1027.

——, P. J. Kocin, R. A. Peterson, C. H. Wash and K. F. Brill, 1984: The Presidents' Day cyclone of 18–19 February 1979: Synoptic overview and analysis of the subtropical jet streak influencing the pre-cyclogenetic period. *Mon. Wea. Rev.*, **112,** 31–55.

——, D. Keyser, K. F. Brill and C. H. Wash, 1985: The Presidents' Day cyclone of 18–19 February 1979: Influence of upstream trough amplification and associated tropopause folding on rapid cyclogenesis. *Mon. Wea. Rev.*, **113,** 962–988.

——, R. A. Petersen, K. F. Brill, P. J. Kocin and J. J. Tuccilo, 1987: Synergistic interactions between an upper-level jet streak and diabatic processes that influence the development of a low-level jet and a secondary coastal cyclone. *Mon. Wea. Rev.*, **115,** 2227–2261.

Whitaker, J. S., L. W. Uccellini and K. F. Brill, 1988: A model-based diagnostic study of the rapid development phase of the Presidents' Day cyclone. *Mon. Wea. Rev.*, **116,** 2337–2365.